PROGRESS IN SENSITIVE MID-INFRARED SPECTROSCOPY OF COOLED MOLECULAR IONS

BY

COURTNEY N. TALICSKA

THESIS

Submitted in partial fulfillment of the requirements
for the degree of Master of Science in Chemistry
in the Graduate College of the
University of Illinois at Urbana-Champaign, 2016

Urbana, Illinois

Adviser:

Professor Benjamin McCall

Abstract

The spectroscopic investigation of molecular ions is key to facilitating a better understanding of chemical and physical processes that occur both here on Earth and among distant stars. However, numerous challenges are encountered when attempting to study these highly reactive species in the laboratory that can only be overcome by the most sensitive spectroscopic techniques. This thesis discusses the first implementation of concentration-modulated noise-immune cavity-enhanced optical heterodyne molecular spectroscopy (cm-NICE-OHMS) on a continuous gas-flow pinhole supersonic expansion discharge source for the study of cooled molecular ions. The instrument, which began as a difference-frequency generation (DFG) based system, is upgraded to include a continuous-wave optical parametric oscillator (OPO) easily tunable from 2.5−4.6 μm. With the implementation of the OPO the system demonstrates a noise equivalent absorption of $\sim 1 \times 10^{-9}$ cm^{-1}. The effectiveness of cm-NICE-OHMS is tested through the acquisition of transitions of H_3^+ and HN_2^+. This study provides confirmation that the source produces H_3^+ rotationally cooled to 80−120 K, while the more efficiently cooling HN_2^+ ion demonstrates a temperature of $\sim$29 K for low rotational states. Further improvements are discussed that will enable cm-NICE-OHMS to reach its full potential for the detection of molecular ions formed in supersonic expansion discharges. Additionally, the current and future status of molecular ion spectroscopy is discussed, and potential molecular ion targets are highlighted to provide direction for investigations of ions of fundamental and chemical importance.

To Mom, Dad, and Josh.

Acknowledgments

I would like to thank my advisor, Benjamin McCall, for his support and guidance over the past few years. He has been a source of great knowledge and through his mentorship I have learned to think more deeply about scientific challenges. I would also like to thank all of the members of the McCall lab for their expertise and the insight they have provided in the many challenges laboratory work presents. I especially thank Michael Porambo for his guidance during my first two years in the lab, under his mentorship I gained the confidence and skills necessary to continue on with the project after his graduation. His demeanor in the lab made the difficulties encountered in day-to-day research manageable, and together we gained momentum from each small victory.

I would not be where I am today without the help of my family and friends. To Jordan, Michaela, and Nicole: thanks for the coffee breaks, movie nights, and talks that have helped to make graduate school fun. To everyone I have met here, and to those I have known for many years, thank you for always being willing to talk and provide a laugh when things get tough. Mom and Dad, thank you for the never ending support you have always given me and, I know, always will. Josh, thanks for always being only a phone call away and providing perspective whenever tunnel-vision sets in. Finally, to the rest of my family: I thank each and every one of you for your support throughout the years. Thank you, all, for the good times we have shared − I look forward to many more to come.

Table of Contents

Chapter 1

Molecular Ions and NICE-OHMS

1.1 The Importance of Molecular Ions

Molecular ions are integral to chemical processes we encounter routinely in life, including combustion [1, 2]. As such, a better understanding of these species could be the key to developing more efficient, cost-effective combustion engines. Molecular ions also serve as key components of atmospheric processes that uphold Earth as an inhabitable environment [3]. The prevalent role of molecular ions as reactive intermediates in many chemical and physical terrestrial processes stresses the desire for a better understanding of these species through theoretical and experimental methods.

Beyond our physical reach, molecular ions are known to play a large role in the chemistry of the interstellar medium (ISM). In the low densities of interstellar space, long-range interactions between ions and neutrals initiate a rich chemistry that has helped to shape our universe [4, 5]. From a theoretical viewpoint, molecular ions often serve as the simplest systems on which to test and verify *ab initio* methods. Here, comparison between theoretical predictions and experimental results acts iteratively to improve the accuracy of calculations for simple systems before applying these methods to more complex systems. It is up to spectroscopists to take these low accuracy predictions and improve experimental measurements to enable better-developed *ab initio* methods for continually larger molecular systems.

1.2 Molecular Ion Spectroscopy

Spectroscopy remains the principal tool used to investigate the properties of molecular ions, with mid-IR spectroscopy providing a distinct advantage. While spectroscopy performed in the near-IR spectral region is largely limited to overtones and combination bands of molecular transitions, the mid-IR provides access to fundamental absorptions that are orders of magnitude more intense. Additionally, nearly all ions of interest have fundamental transitions in the mid-IR.

As it takes more energy to make a molecule vibrate than rotate, excitation of a normal vibrational mode of a molecule results in the population of many rotational states. High-resolution rotational-vibrational (rovibrational) mid-IR spectroscopy, which resolves the rotational fine-structure of vibrational bands, is a powerful tool used to examine the rotational structure of strong fundamental vibrations. From the information obtained via this method it is possible to determine rotational constants and molecular structure [6]. Additionally, when conducted at sufficiently high precision this method also allows for the indirect determination of pure rotational transition frequencies through the use of combination differences [7].

Many challenges arise when investigating molecular ions in the laboratory. Ions are formed in small abundances in laboratory plasmas and successful detection requires the use of highly sensitive spectroscopic techniques. In addition, neutral species are orders of magnitude more abundant, and a means of discerning the ion signal from the largely neutral background must be achieved. Finally, the high temperatures inherent to traditional laboratory ion sources prompts the population of many quantum states and result in dilute, complex spectra.

1.3 Cooled Molecular Ions

Ion sources capable of producing high densities of ions for study in the laboratory have long been realized in hollow cathode and positive column discharge sources [8–10]. However, even when cryogenically cooled the internal temperatures of ions formed by such sources are on the order of 100 K, at which temperatures many rotational states remain populated. Weakened spectral signals then result from the decreased population of any one state. Cooling molecular ions to low temperatures overcomes this problem by concentrating population into low-energy states, thus strengthening low-lying rotational transitions and reducing the spectral complexity of large systems.

Molecular ions cooled to temperatures of tens of kelvin can be produced through the coupling of electric discharges to supersonic expansions. Here, a precursor gas is seeded in a carrier gas at high pressure and forced through a small orifice into vacuum. Striking a discharge along the length of the expansion channel allows ions formed in the nozzle of the expansion to be cooled to low temperatures as the ionized gas expands adiabatically into vacuum. In addition to producing cold molecular ions, supersonic expansion discharges have the unique ability to efficiently produce ions that other sources cannot, including primary and cluster ions [11–16].

The effect of cooling on the intensities of rovibrational transitions is demonstrated in Figure 1.1, where the ν_1 band of HN_2^+ centered near 3234 cm^{-1} has been simulated using PGopher [18]. An improved relative intensity for low J transitions is clearly seen at lower temperature (30 K), whereas the higher temperature simulations show the population of more quantum states with a weakened intensity of each individual state. While cooling ions to low temperatures efficiently concentrates ion population into low rotational states and strengthens low-lying transitions, the stringent pumping demands required for expansion discharges restrict such sources to small path lengths and limits the sensitivity with which ions formed by these sources can be detected.

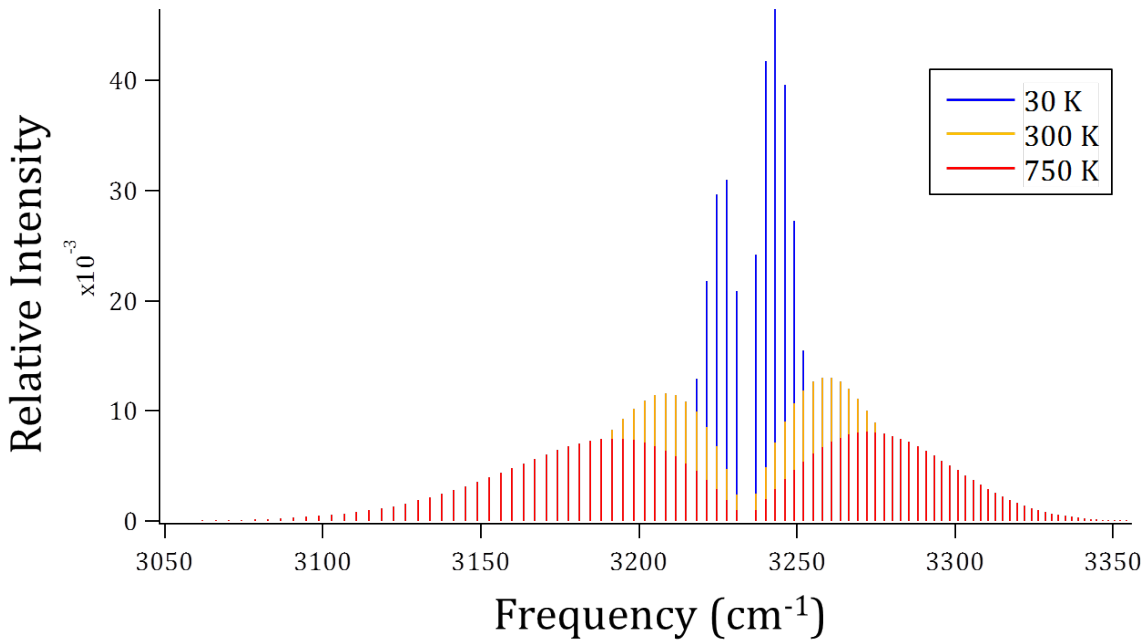

Figure 1.1: Simulations of the ν_1 band of HN_2^+ centered near 3234 cm^{-1} at 30 K, 300 K, and 750 K. Simulations were performed using PGopher with upper and lower state constants taken from Nakanaga et al. [17, 18].

1.4 NICE-OHMS

Direct absorption spectroscopy (DAS) provides the most straightforward method for the spectroscopic investigation of molecular species. However, experimental implementation of this method often results in sensitivities that are orders of magnitude above the theoretical shot noise limit due to noise contributed by the light source. To improve the sensitivity of DAS, frequency modulation spectroscopy (FMS) has been demonstrated as an effective means of noise reduction and has enabled sensitivities down to 10^{-6} $Hz^{-1/2}$. The sensitivity of DAS has also been improved by increasing the strength of the observable signal through the use of an optical cavity. Here, techniques such as cavity ring-down spectroscopy (CRDS) typically exhibit sensitivities on the order of 10^{-8} $Hz^{-1/2}$ [19].

Superior spectroscopic sensitivity can be achieved through the combination of FMS and cavity enhancement. The merging of the strengths of these techniques is key to the high

sensitivities achieved by noise-immune cavity-enhanced optical heterodyne molecular spectroscopy (NICE-OHMS), where heterodyne detection for the reduction of technical noise is combined with cavity enhancement to increase the sample pathlength interaction. This technique avoids the frequency-to-amplitude noise common in cavity-enhanced techniques by matching the heterodyne frequency to an integer multiple of the free spectral range (FSR) of the optical cavity. This allows all components of the frequency-modulated (fm) triplet to be transmitted through the cavity in an identical manner. Detection of the transmitted signal is then achieved through demodulation of the sum of the beat notes of the carrier with the upper and lower sidebands. In the absence of intracavity absorption or dispersion the sidebands are equal in magnitude and opposite in phase so that the beat notes exactly cancel, yielding no net signal and making NICE-OHMS a zero-background technique [19].

NICE-OHMS has demonstrated sensitivities down to 1×10^{-14} cm^{-1} Hz$^{-1/2}$ for detection of neutrals in the near-IR [20]. This model sensitivity was achieved at 1.064 μm with a cavity finesse of 100,000, which required an ultrastable laser (1 mHz) be used as the excitation source [20]. NICE-OHMS in the near-IR benefits from a variety of well-developed light sources and detectors that are readily available. With a considerable lag in analogous technology in the mid-IR, it follows that implementations of mid-IR NICE-OHMS have been less prevalent than those of its near-IR counterparts. Specifically, smaller detection bandgaps, slower detectors, and weaker light sources make it more difficult to implement this technique in the mid-IR. Nevertheless, successful implementations of NICE-OHMS in the mid-IR have been demonstrated [21, 22].

Chapter 2

Mid-Infrared NICE-OHMS of a Supersonic Expansion Discharge

2.1 Supersonic Expansion Discharge

The design of the continuous gas-flow supersonic expansion (SSE) source has been described in detail in an earlier publication [16]. While the cathode used in this work retains the dimensions and shape described there (a trumpet-flared pinhole with 1.0 mm starting and 2.4 mm ending inner diameters), it has been replaced by one machined from tungsten (previously stainless steel) in order to further improve the lifetime of the source. It has been found previously that the density of H_3^+ ions produced varies with the current supplied to the source ($10^{10}-10^{12}$ cm^{-3} for 30−120 mA), and HN_2^+ is expected to be formed in similar quantities in a predominantly hydrogen expansion [16].

To form cooled H_3^+, pure H_2 is flowed through the main pipeline of the source at backing pressures ranging from 30−36 psig. It should be noted that at backing pressures below 30 psig significant cooling of H_3^+ is not consistently observed. HN_2^+ is formed in the source from a mixture of hydrogen and nitrogen gas each regulated to control their respective gas flow rates and combined before being flowed into the source. Here, equal backing pressures (34 psig H_2, 34 psig N_2) gives the strongest HN_2^+ signal. While scanning H_3^+ and HN_2^+, chamber background pressures of 600−750 mTorr (as recorded by a Varian 531 thermocouple gauge tube sensor) are typically used as this range of pressures gives the most pronounced barrel-

Sections 2.1, 2.3, and 2.5−2.7 have been submitted for publication in Review of Scientific Instruments with authors C. N. Talicska, M. W. Porambo, A. J. Perry, and B. J. McCall.

shock structure and strongest ion signal. The background pressure is easily adjusted by partially closing the gate-valve on the expansion chamber.

2.2 DFG NICE-OHMS Instrument

The first instance of NICE-OHMS applied to a supersonic expansion discharge source was realized through the use of a previously designed broadly tunable mid-IR NICE-OHMS spectrometer [22]. This instrument utilized difference-frequency generation (DFG) between a fixed-wavelength Nd:YAG (1064 nm) and tunable Ti:Sapph (∼700-1100 nm) laser to produce 160−200 μW of mid-IR light tunable from 2.8−4.8 μm. The experimental setup is shown in Figure 2.1 and is detailed further in the work of Porambo et al. [22].

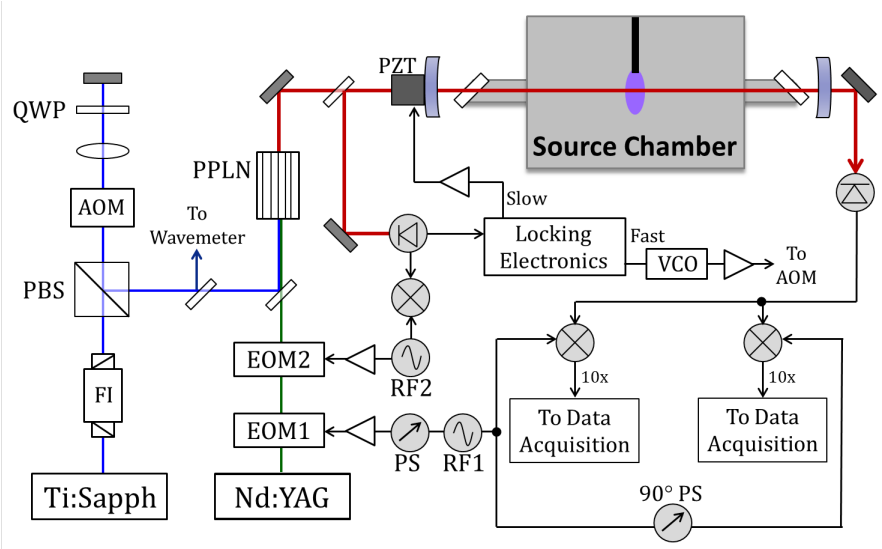

Figure 2.1: Block diagram of the DFG NICE-OHMS instrument. AOM: acousto-optic modulator; EOM: electro-optic modulator; FI: Faraday isolator; PBS: polarizing beam splitter; PPLN: periodically-poled lithium niobate; PS: phase shifter; PZT: piezoelectric transducer; QWP: quater wave plate; VCO: voltage-controlled oscillator

Due to noise in the system and the limited power of the DFG, efforts to observe H_3^+ utilizing DFG NICE-OHMS yielded no signal. Careful mode-matching improved the amount of light coupled into the cavity, thus increasing the amount of light interacting with the discharge and reaching the transmission detector. However, noise in the system still impeded

a detection of even H_3^+ and it was necessary to devise a method to improve the sensitivity of the instrument.

2.3 Concentration-Modulated NICE-OHMS

The sensitivity of spectroscopic techniques used to probe molecular ions in an expansion discharge source can be improved through electrical modulation of the source, which results in a periodically varying concentration of ions. Lock-in detection at the source modulation frequency then provides high selectivity of the desired ion signal while rejecting much of the unwanted noise in the system. Davis et al. demonstrated improved sensitivity of a direct absorption technique used to probe an expansion discharge source using this method [15]. Despite its ability to enable improved detection of molecular ions, until this work modulation of an expansion discharge had not yet been applied to the sensitive NICE-OHMS technique.

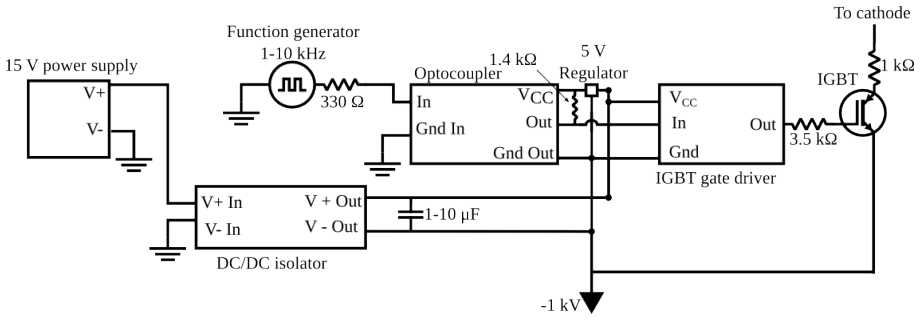

Figure 2.2: Diagram of the custom high-voltage circuit used to modulate the discharge.

To implement modulation of the supersonic expansion discharge source a custom high-voltage modulation circuit was designed in collaboration with Thomas Houlahan Jr. of the Electrical and Computer Engineering Department. This circuit, shown in Figure 2.2, uses an optoisolator (Avago Technologies ACNV2601-000E) to separate the low-voltage input of a function generator from the high-voltage power supply. The output of the optoisolator is fed into a gate-driver (ON Semiconductor MC33153PG) for an insulated-gate bipolar transistor (IGBT) (Infineon IHW30N160R2) before being output through the ballast resistor to the

cathode of the source. Performance of the modulation circuit was assessed for modulation frequencies ranging from ∼25 Hz−85 kHz. The circuit was found to break down in the low frequency regime (<25 Hz) due to high transient voltage spikes.

Integration of the source modulation with the DFG NICE-OHMS instrument was achieved by sending the output of the electronic mixers used to isolate the NICE-OHMS signals into a pair of lock-in amplifiers referenced to the trigger applied to the source. Thus, in this setup, the ion signal is first demodulated at the heterodyne frequency (∼100 MHz) and then at the source modulation frequency (∼1 kHz). This concentration-modulated (cm) NICE-OHMS instrument, which enabled the detection of H_3^+ and HN_2^+, is detailed in Figure 2.2.

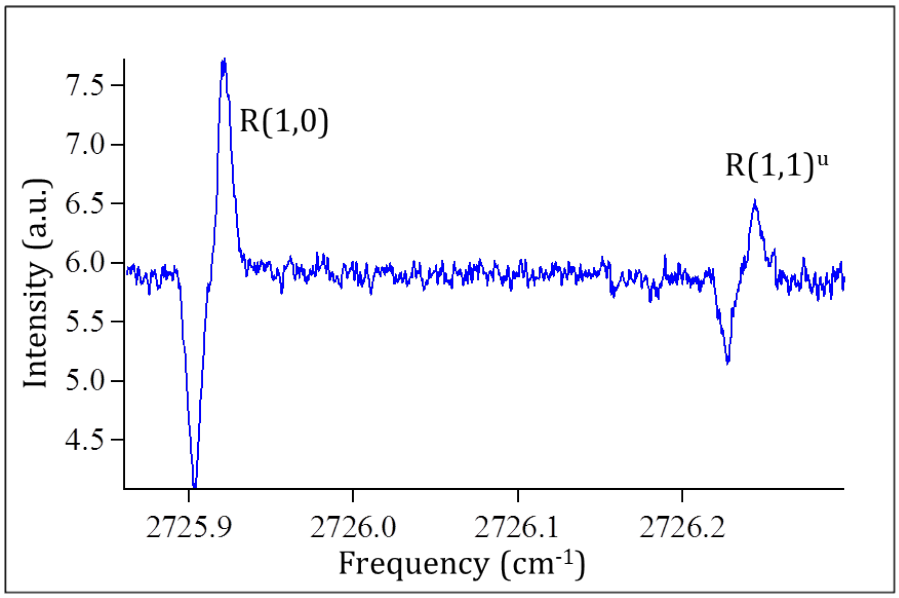

Figure 2.3: A scan of the R(1,0) and R(1,1)^u transitions in the ν_2 fundamental band of H_3^+ near 2726 cm^{-1} using DFG cm-NICE-OHMS.

To ensure cm-NICE-OHMS can be accurately used to determine the extent of cooling of molecular ions formed by the source, the rotational temperature of H_3^+ was determined and compared to that of H_3^+ formed in the same source but analyzed previously by CRDS [16]. As in the CRDS analysis, the rotational temperature was estimated by the ratio of the normalized intensities of the R(1,0) and R(1,1)^u transitions in the ν_2 fundamental band near 2726 cm^{-1}. A scan of these transitions is given in Figure 2.3 and is representative of the

typical signal-to-noise achieved for R(1,0) of H_3^+ using this instrument. The estimated temperature of 80−120 K was further verified through a Boltzmann analysis including R(2,2)^l, and agrees well with the temperature of 80−110 K obtained by CRDS [16].

2.4 A More Powerful Light Source

While DFG cm-NICE-OHMS was successful in enabling the detection of H_3^+ and HN_2^+, the limited power and complexity of the instrument left much room for improvement. The poor noise rejection of the sensitive mid-IR detector required to detect the μW of DFG power transmitted through the cavity greatly limited the signal-to-noise of transitions acquired using this method. In addition, drastic wavelength changes required changing poling periods in the PPLN crystal, which often led to loss of the DFG and long instrument downtimes due to the complexity of the optical layout. To overcome these limitations a commercial turnkey optical parametric oscillator (OPO) was integrated with cm-NICE-OHMS. This new light source is capable of producing 100s of milliwatts of mid-IR light and is easily tunable from 2.5−4.6 μm.

The OPO used to improve the cm-NICE-OHMS instrument was concurrently shared between two projects. As such, the OPO was mounted on a separate optics table, and a method of transmitting the idler beam to the table surrounding the SSE had to be devised. First attempts to achieve this were done using a long mid-IR fiber (11 m, 100 μm core diameter InF_3, ThorLabs) strung through runners above the two tables. A mode-matching telescope was used to shape the idler beam before being launched into the fiber, and another telescope was positioned after the exit for optimal mode-matching into the cavity surrounding the source. With the full force of the OPO incident on the fiber, ∼300 mW of light was transmitted to the SSE table.

With this method it was possible to improve the amount of light reaching the optical cavity to 100s of mW, nearly three orders of magnitude greater than that achieved using the

DFG light source (140−200 μW). However, the mode-structure of the light coupled into the cavity was found to change over time and with movement of the fiber as illustrated by beam profile measurements as shown in Figure 2.4. The changing mode-structure is inherent to the large core of the fiber (∼100 μm), which allows multiple modes to propagate, and was extreme enough to severely change the cavity-mode strength even over a small scan window. This changing mode-structure drastically interfered with the efficiency of the laser-to-cavity lock, and the use of the mid-IR fiber as a means of transmitting the idler to the SSE table was subsequently abandoned.

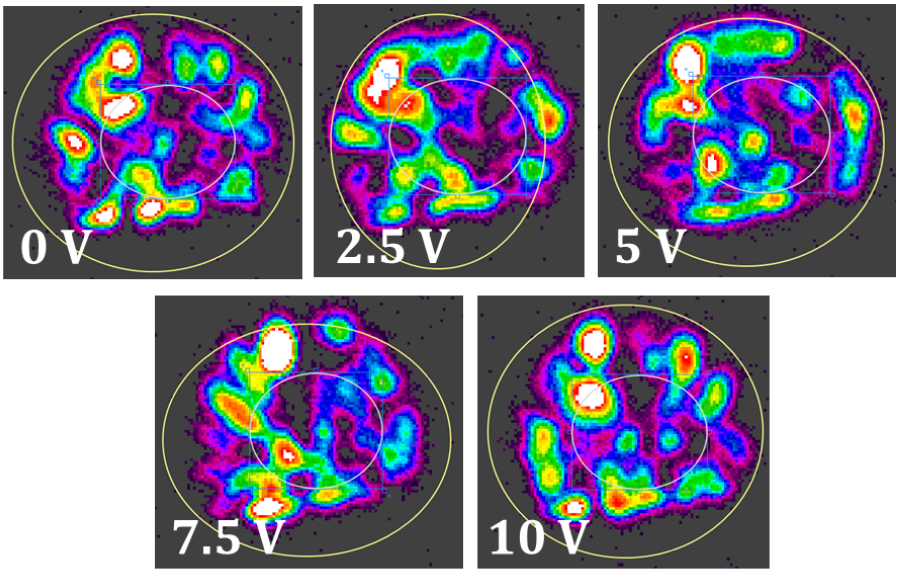

Figure 2.4: Beam profile measurements of the output of the mid-IR fiber over a 10 V (∼5 GHz) scan of the pump laser of the OPO. Drastic changes in the mode-structure are seen even for small scan windows (7.5−10 V, ∼1.25 GHz)

Instead, the idler beam was directed over free-space from the OPO to the SSE table as shown in Figure 2.5. To ensure safe direction of the idler across the ∼10 ft. of open space, the beam was directed through a 3-inch diameter PVC pipe held in place by two custom-made Unistrut supports that stood on the lab floor. In this design, the idler passes through only one mode-matching telescope designed to ensure efficient coupling into the optical cavity. Thus, more light reaches the transmission detector than in the mid-IR fiber setup.

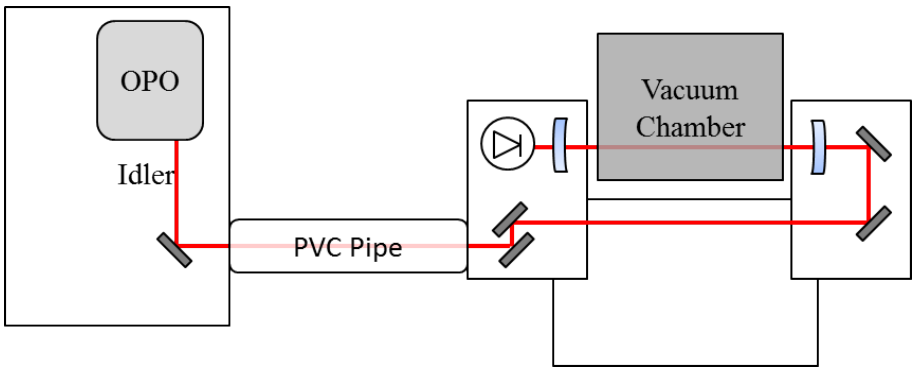

Figure 2.5: Block diagram of the free-space OPO setup.

The free-space setup is sensitive to the relative positions of the two individual optical tables, and significant perturbations result in changes to the transmitted cavity power. However, after the cavity is optimized, the system is robust enough to allow for a full day of uninterrupted scanning provided no drastic changes are made to components on the two tables. With this setup scans of H_3^+ and HN_2^+ were successfully obtained.

2.5 OPO cm-NICE-OHMS Instrument

A block diagram of the OPO cm-NICE-OHMS instrument is given in Figure 2.6. The OPO simplifies the cm-NICE-OHMS instrument considerably as many of the free-space optics required in the DFG setup are replaced with fiber components. In this setup a ytterbium-doped fiber laser is phase-modulated by a fiber electro-optic modulator (EOM) to produce RF sidebands for heterodyne detection and Pound-Drever-Hall (PDH) locking. The modulated light is amplified to 10 W before being used to pump a singly-resonant OPO (Acculight Argos 2400 SF). As a result, the heterodyne ($\sim$106 MHz) and PDH locking (2$-$10 MHz) sidebands are imprinted onto the idler beam (2.5$-$4.6 μm).

The idler beam is then coupled into the $\sim$1.4 m cavity placed symmetrically about the source chamber such that the idler passes perpendicularly through the axis of the expansion. Light reflected from the cavity is picked off using a CaF_2 window and focused onto a fast InSb detector (Kolmar KISDP-0.5-J1/DC, 30 MHz bandwidth), where it is then demodulated at

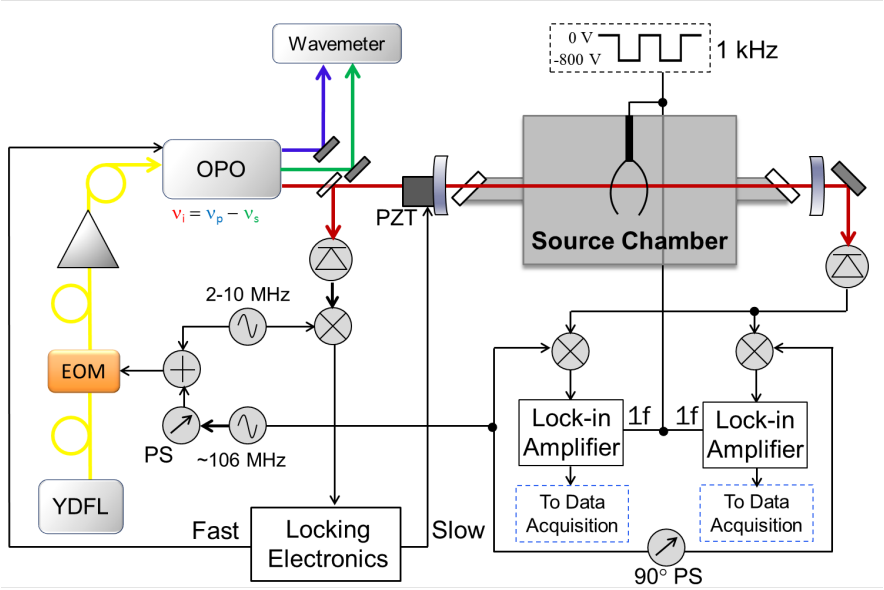

Figure 2.6: Block diagram of the cm-NICE-OHMS instrument. EOM: electro-optic modulator; OPO: optical parametric oscillator shown with pump (P), signal (S), and idler (I) beams; PS: phase shifter; PZT: piezoelectric transducer; YDFL: Ytterbium-doped fiber laser

the PDH locking frequency. Slow locking corrections (<70 Hz) are made to the cavity length by a piezoelectric transducer (PZT) attached to one of the cavity mirrors, and fast corrections (0.07−10 kHz) are sent to a PZT attached to one of the signal cavity mirrors within the OPO head.

Transmitted cavity light is focused onto a fast photodiode (Vigo PVM-10.6-1, ∼125 MHz bandwidth) before being demodulated at ∼106 MHz by a pair of electronic mixers set to be 90° out of phase with each other. To implement cm-NICE-OHMS, an additional layer of modulation is added through electrical modulation of the discharge as discussed in Section 2.3. The periodically varying ion signal is then recovered by sending the outputs of the electronic mixers used to isolate the NICE-OHMS signals to a pair of lock-in amplifiers referenced to the modulation frequency applied to the source. As with DFG cm-NICE-OHMS, the output of the lock-in amplifiers are then fed into a custom-made program for data acquisition.

2.6 Characterization of the Source using OPO cm-NICE-OHMS

Previous characterization of the unmodulated supersonic expansion discharge source using CRDS revealed a rotational temperature for H_3^+ of 80−110 K [16]. With its larger rotational constants (B = 43.5605 cm^{-1}, C = 20.6158 cm^{-1} [23]) and thus lower density of rotational states, H_3^+ does not cool as efficiently in a supersonic expansion as HN_2^+ (B = 1.5539 cm^{-1} [24]). Due to its capacity to cool more efficiently, HN_2^+ was used in this work to investigate the cooling abilities of the source using concentration-modulated NICE-OHMS.

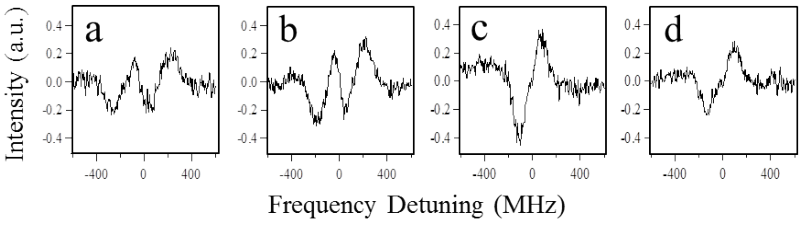

Figure 2.7: Scans of the R(2) transition of the ν_1 fundamental band of HN_2^+ taken 0.5 cm (a), 1.5 cm (b), 2.0 cm (c), and 2.5 cm (d) from the source nozzle, shown with approximate frequency detunings from linecenter. All scans were obtained at backing pressures of 34 psig, 750 mTorr chamber pressure, a source modulation frequency of 1 kHz, and a current of 110 mA.

To assess the rotational cooling of HN_2^+ in the source, transitions in the ν_1 fundamental band of HN_2^+, centered near 3234 cm^{-1}, were recorded. All scans used in the analysis were obtained at just over 2 cm downstream of the source nozzle. At distances closer to the expansion nozzle a peculiar lineshape was observed, as shown in Figure 2.7 and discussed in detail elsewhere [25]. An unprocessed scan of each transition is given in Figure 2.8. These scans were taken at a detection phase of ∼160° as fit by a lineshape model taken from equations 1−3 in the work of Foltynowicz et al. [19]. The acquired scans were then smoothed using a 10-point boxcar averaging algorithm. The average of peak-to-peak intensities from at least three boxcar-smoothed scans of each line were normalized to their respective transition dipole moments as calculated in Townes et al. [26]. Due to a dead spot in the frequency

coverage of the OPO, the R(1) transition was not recorded.

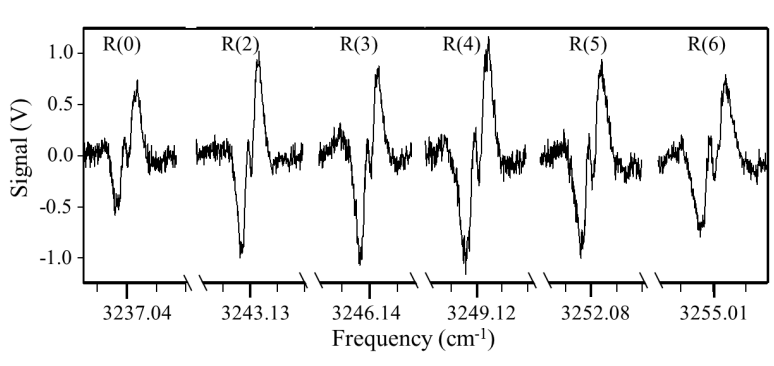

Figure 2.8: Scans of the R(0), and R(2−6) transitions of the ν_1 fundamental band of HN_2^+. Each tick on the frequency axis represents 0.01 cm^{-1}.

Figure 2.9 shows the Boltzmann analysis of these normalized intensities, plotted against lower state energies calculated using the rotational constants reported by Kabbadj et al. [24]. The two distinct slopes are representative of the non-equilibrium nature of the expansion as has been reported in similar analyses by Xu et al. [13] and Louviot et al. [27]. Analyzing the slope of the low J transitions ($J \leq 3$) gives a rotational temperature of ∼29 K. This temperature is similar to the 33 K rotational temperature determined for low J transitions of HN_2^+ in a corona slit nozzle discharge expansion reported by Xu et al. [13] and also agrees well with the 25 K rotational temperature reported by Anderson et al. for low J transitions of this ion in a pulsed slit expansion discharge [14].

Utilizing equations detailed in the work of Ma et al. the NICE-OHMS saturation parameter associated with the work presented here has an upper bound of ∼6 [28]. At this degree of saturation, the effect on the peak-to-peak intensity of the absorption Doppler profile is demonstrated to be <5%, and is not large enough to alter the temperature calculated by the Boltzmann analysis. To further support the determined temperature, this analysis was repeated with the intensities of the predominantly dispersion-phase channel, which demonstrate peak-to-peak intensities unaffected by this level of saturation. The temperatures calculated from the absorption and dispersion-phase channels agree, substantiating the rotational temperature of ∼29 K calculated for HN_2^+ formed in the expansion.

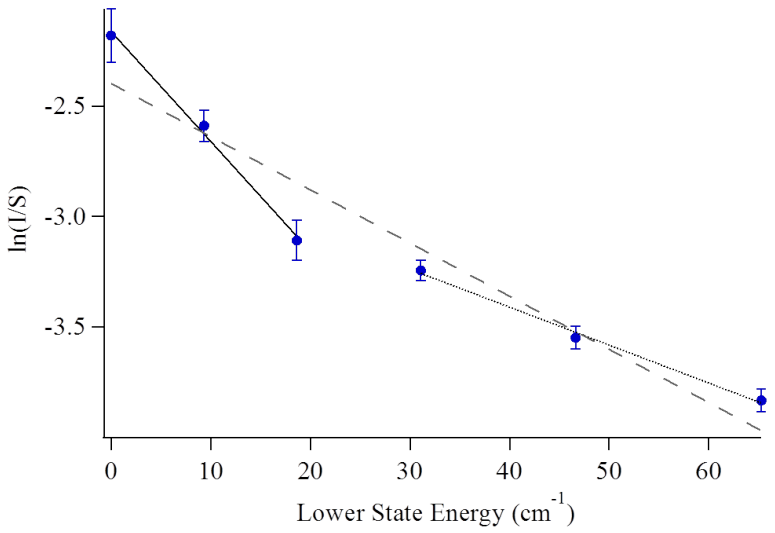

Figure 2.9: A Boltzmann diagram of the rotational distribution of HN_2^+ shown with 2σ error bars. The fit to the low J (R(0), R(2), and R(3), solid line) gives a temperature of $\sim$29 K, while the fit to the high J values (R(4)$-$R(6), dotted line) gives a temperature of $\sim$84 K. The dashed line corresponds to a fit to all J values.

The lower temperature obtained for HN_2^+ ($\sim$29 K) compared to H_3^+ (80$-$110 K [16]) in the same continuous gas-flow supersonic expansion discharge source was anticipated due to the higher density of rotational states associated with low J values of HN_2^+. The low temperature achieved for HN_2^+ in this work also agrees well with those achieved for comparable ions in studies of a concentration-modulated pulsed-gas slit expansion discharge where HD_2O^+ and H_2DO^+ were cooled to 34 K and 40 K, respectively [29,30]. The cooling abilities of the source as verified by the concentration modulated NICE-OHMS technique are thus in accordance with the cooling achieved in expansion discharges probed by other spectroscopic methods.

The high J transitions (J $\geq$ 4) indicate a warmer temperature of $\sim$84 K, similar to the phenomenon reported by Xu et al. where higher J transitions of HN_2^+ gave warmer temperatures [13]. The observed increase in temperature for high J levels is an expected result of larger energy spacings among these levels which results in less efficient cooling through rotation-to-translation energy transfer. As shown by the dashed line in Figure 2.9, a fit to all J values does not encapsulate the normalized intensities of all J levels, even when including 2σ errors in the measurements. This is indicative of the non-equilibrium nature of

supersonic expansions and highlights the need for separate fits to the low and high J values of the Boltzmann analysis.

The FWHM of HN_2^+ scans acquired in this work is $\sim$100$-$110 MHz as supported by the Doppler-broadened lineshape model of Foltynowicz et al. [19]. As the FWHM of HN_2^+ is already on the order of the heterodyne sideband spacing, further optimizing the sideband spacing is not expected to yield a significant increase in the acquired signal. For ions with larger FWHMs (such as H_3^+) the sideband spacing may be adjusted to optimize the obtained signal, but is limited by the fact that the heterodyne frequency must be an integer multiple of the free-spectral-range of the cavity and must be within the bandwidth of the mid-infrared detector used to recover the transmitted signal.

Improved detection of ions formed by the source may be achieved by increasing the source modulation frequency, further reducing noise in the system. Throughout the course of this study scans were obtained at a source modulation frequency of $\sim$1 kHz. At higher frequencies the source current was found to take time to stabilize during the plasma "on"-cycle as evidenced by monitoring the source current using a Hall-effect sensor placed just before the source. Resolving this current instability would allow the source modulation frequency to be limited only by the expansion of ions through the laser probe region. For an expansion velocity of $\sim$2 km/s and a beam diameter of $\sim$2 mm, the theoretical upper limit to this modulation would be $\sim$500 kHz barring any limits due to the modulation circuit and lock-in amplifier bandwidth [15].

2.7 Conclusions

The work presented here highlights the successes of the first implementation of concentration-modulated NICE-OHMS for the investigation of molecular ions formed in a supersonic expansion discharge source. This technique has been used to characterize the cooling of both H_3^+ (80$-$120 K) and HN_2^+ ($\sim$30 K) formed by the source, with HN_2^+ serving as a good

approximation of the low-temperature limit for efficiently cooling molecular ions. This low temperature tailors this spectroscopic setup toward the investigation of larger molecular ions which would exhibit dilute, congested spectra in higher-temperature ion sources.

The main advantage of this instrument over previously designed FMS, CRDS, and multi-pass setups is the potential for achieving a higher sensitivity through the combination of cavity-enhancement, heterodyne detection, and lock-in detection. Here, the performance of the concentration-modulated NICE-OHMS spectrometer is characterized by the noise equivalent absorption sensitivity. This value is derived from the rms of the baseline noise present in the scans and, after correction for amplification in the detection train, is found to be $\sim 1 \times 10^{-9}$ cm^{-1}. This sensitivity is nearly two orders of magnitude better than that achieved by CRDS of a slit-expansion discharge (2×10^{-7} cm^{-1}) [31]. The signal-to-noise ratio of the observed spectra may be improved by increasing the sample pathlength (through the use of a slit expansion and/or improvements to the cavity finesse). Additionally, reducing noise by increasing the source modulation frequency, and by finding and eliminating sources of noise in the system, will further improve the effectiveness of this instrument.

To fully realize the potential of concentration-modulated NICE-OHMS of a supersonic expansion discharge source for the investigation of ions formed in less abundance than HN_2^+, it will be necessary to continue to improve the sensitivity of the instrument. Increasing the sample pathlength through the use of a slit geometry could easily improve the sensitivity by a factor of 3 or 4, as slits with lengths of $3-4$ cm have previously been used in expansion discharges [15]. In addition, the cavity finesse is currently limited by the presence of Brewster's windows on the expansion chamber. If a method of directly mounting the cavity mirrors to the chamber can be realized, the finesse could be improved to the limit of the reflectivity of obtainable mirrors and the locking bandwidth of the system. However, this improvement is made difficult by the mechanical vibrations of the Roots blower pump. Overall, the instrument described here makes important steps towards the more sensitive detection of molecular ions formed in supersonic expansion discharges, and can be further improved

upon to take full advantage of the concentration-modulated NICE-OHMS technique.

Chapter 3

The Past and Future of Molecular Ion Spectroscopy

Noise-immune cavity-enhanced optical heterodyne velocity modulation spectroscopy, or NICE-OHVMS, was developed in the McCall lab and has enabled precise determination of transition line-centers for numerous molecular ions including HeH^+, H_3^+, HCO^+, and OH^+ [7,21,32–34]. As the name implies, this method retains the high sensitivity achieved through the pathlength enhancement and heterodyne detection of NICE-OHMS, but adds ion-neutral discrimination by integrating velocity modulation of ions formed in a positive column discharge source. The high sensitivity of NICE-OHVMS will enable the successful detection of molecular ions that have evaded spectroscopists thus far. This chapter summarizes many of the molecular ions that have already been studied, as well as those for which NICE-OHVMS may pave the way for high-resolution study. In addition, future spectrometers utilizing a quantum cascade laser (QCL) may allow for the study of low-frequency vibrational bands near 8.5 μm. While not an exhaustive search, the ion targets and references provided herein serve as a starting point for the experimentalist looking to further the cause of ion spectroscopy in the mid-IR.

3.1 Hydrogen/Deuterium Ions

One of the most widely studied hydrogen ions, H_3^+, was discovered more than 100 years ago by J. J. Thomson in a hydrogen discharge [35]. H_3^+ is known to be the dominant positively charged ion present in hydrogen plasmas, and its rovibrational spectrum was first observed in 1980 [36,37]. Theoretical studies have since successfully reproduced the obtained

laboratory spectra and have predicted the frequencies of new lines to guide future laboratory studies [36]. Beyond Earth's atmosphere H_3^+ was first detected by emission spectroscopy in Jupiter's aurora, and is known to be responsible for much of the chemistry that occurs in interstellar space [4, 38]. The importance of H_3^+ is extremely far-reaching and, as such, this ion continues to be the subject of spectroscopic investigations to this day.

Hydrogen cluster ion systems have been demonstrated to exist mostly as H_3^+ ions surrounded by H_2 molecules [39]. These systems often serve as benchmarks for the development of theoretical methods focused on molecular structure, energy, and dynamics. Additionally, these ions are of interest in modeling the nucleation dynamics of planetary and interstellar conditions, and may be useful as a means of storing energy [40, 41]. Odd-n H_n^+ clusters are known to be more stable than their even-n counterparts, with hydrogen clusters up to n=47 having been observed for the odd-n species [40]. Further spectroscopic investigation of these cluster ions is necessary to fully characterize the behavior and dynamics of these systems, as well as to provide benchmarks for further improvements to theoretical methods.

H_5^+ and Isotopologues

First discovered more than fifty years ago, H_5^+ has long been studied by experimental and theoretical methods [42]. From a fundamental view, this ion serves as a comparatively simple system through which the spectroscopic consequences of large amplitude motions can be explored [43]. In its ground vibrational state, H_5^+ is best visualized as a symmetric proton-bound dimer wth D_{2d} symmetry with the central proton equally shared between two almost freely rotating H_2 molecules [40, 43, 44]. The "floppy" nature of this ion makes exact quantum calculations of the IR spectrum unworkable, but several *ab initio* studies utilizing high-level theoretical methods have predicted the frequencies of several vibrational modes of this ion [43, 45–47].

In order to gain a better understanding of H_5^+, experiment and theory have worked together for many years, iteratively predicting and attempting assignments of vibrational bands [43–46, 48]. The shared proton mode has been observed near 1180 cm^{-1} (1184 cm^{-1}

predicted by theory) [44]. Low-resolution experimental studies have utilized action spectra, free electron lasers, and IR multi-photon dissociation spectroscopy to show the existence of further vibrational bands near 2603, 3520, and 3904 cm^{-1} for H_5^+, as well as bands near 2546, 2815, and 3044 for its deuterated counterpart, D_5^+ [39, 44, 45]. The vibrational bands observed for D_5^+ are red-shifted by approximately a factor of $2^{1/2}$, as would be expected for the heavier isotopologue [45]. Furthermore, rotational spectra have been predicted for additional dueterated species of H_5^+ ($H_2D_3^+$, $H_3D_2^+$, H_4D^+), which may help to guide future laboratory searches for this ion [49].

Ion	**Frequency (cm^{-1})**	**Notes**
H_5^+	1180 [44]	Experimental value agrees with 1184 cm^{-1} predicted by theory in this study
	2603 [45]	
	3520 [45]	
	3904 [45]	
D_5^+	1196 [44]	Very weak, theoretical prediction
	2546 [45]	Assigned to ν_8
	2815 [45]	Strongest band
	3044 [45]	Very weak
H_7^+	3982 [41]	3980 cm^{-1} reported by Okumura et al. [39]
D_7^+	2871 [41]	
H_9^+	4033 [41]	4020 cm^{-1} reported by Okumura et al. [39]
D_9^+	2894 [41]	

Table 3.1: Vibrational frequencies of hydrogen and deuterium cluster ions. Unless otherwise noted, reported frequencies are based on experimental observations.

H_7^+, D_7^+, H_9^+, D_9^+

Extending spectroscopic investigations to larger cluster ions will provide further information on the dynamic behavior of these systems, and will provide benchmarks for the further development of theoretical methods for more complex systems. A study done by Okumura et al. in 1985 provides experimental evidence for vibrational frequencies of H_7^+ and H_9^+ near 3980

and 4020 cm^{-1}, respectively [39]. This work utilized electron impact ionization of neutral clusters formed in a molecular beam (10 μm expansion orifice) to generate these ions, which were then trapped in an RF octuple ion trap and examined using a tunable IR laser [39]. The observed frequencies agree well with a later theoretical investigation conducted by Young et al. in which vibrational bands or H_7^+ and H_9^+ were both experimentally and theoretically verified to lie near 3982 and 4083 cm^{-1}, respectively [41]. This observed agreement between experiment and theory provides further validation for using the frequencies predicted by the same study for D_7^+ (2871 cm^{-1}) and D_9^+ (2894 cm^{-1}) as accurate frequencies at which to begin high-resolution searches for these ions [41].

3.2 Carbo-Ions

The work of the Oka Ion Factory provides a good foundation for the spectroscopy of molecular ions containing only carbon and hydrogen atoms, or "carbo-ions". Of particular note is CH_5^+, which was first observed spectroscopically in 1999, but remains unassigned to this day [50]. Previous successes in acquiring and interpreting the spectra of single-carbon carbo-ions include CH_2^+, CH_3^+, and CH_4^+ [51–54]. In the realm of two-carbon species, Oka's group has successfully obtained high-resolution spectra of $C_2H_2^+$ and $C_2H_3^+$ using both positive-column and hollow-cathode discharge cells [55–58]. The vast majority of lines associated with these species have been identified through the analysis of spectral patterns and the observed linewidth (the positive-column studies utilized velocity-modulation spectroscopy (VMS) which provides a degree of mass-information and allows for the discrimination between one and two-carbon species). To be successful in observing and assigning these spectra, it was necessary for the Oka group to work closely with theorists − similar collaborations will likely be necessary for those daring to take on the carbo-ions discussed further below.

Like $C_2H_2^+$, $C_2H_4^+$ and $C_2H_6^+$ are primary ions formed from their neutral parent compound ethylene and ethane, respectively. These ions are expected to be formed in some amount

whenever their parent compound is present, and are likely to be present in hydrocarbon discharges used to study $C_2H_5^+$ and $C_2H_7^+$. Protonated ethylene and protonated ethane join protonated acetylene in the realm of cations existing in two conformers that are close in energy, namely the "classical" and "non-classical" structures [12, 55, 59]. In addition, proton scrambling is hypothesized to occur due to the highly dynamic nature of these species. Evidence of tunneling may be found in high-resolution studies due to the splitting of spectral lines, as was observed for $C_2H_3^+$ [55]. High-resolution and high-precision studies remain necessary to concretely unravel the behavior and structure of these ions.

CH_5^+

The infamous CH_5^+ ion has baffled spectroscopists for years. Upon protonation, the well-defined structure of CH_4 transforms into an extremely floppy system that is remarkably stable. Protonated methane has been known (from mass spectra) to exist since the 1950s, and was even observed spectroscopically in 1999, but a full understanding of the structure and motions of this ion remains unsecured [50,60]. This ion may be thought of as a "protoype of hypercoordinated carbon and of three-center two-electron bonding [61]" due to five equivalent protons continuously scrambling around the central carbon atom [62]. With nearly barrierless proton scrambling, large amplitude motions exist even at very low temperatures, leading to a highly fluxional ion that makes interpreting experimentally obtained spectra exceptionally difficult [60].

An experimental spectrum of CH_5^+ was first obtained by White et al. in 1999 using velocity modulation spectroscopy of a liquid-nitrogen cooled positive column discharge cell [50]. Of the lines observed from $\sim$2770$-$3150 cm^{-1}, lines belonging to other molecular ions inadvertently formed in the CH_4/H_2/He plasma were easily identified (H_3^+, CH_3^+, $C_2H_3^+$, HCO^+, $HCNH^+$, etc.) [50]. This left behind approximately 900 lines with no obvious spectral pattern, many of which are believed to belong to CH_5^+ [50]. In an attempt to gain insight to the behavior of CH_5^+, Huang et al. obtained a jet-cooled spectra of this ion in 2006. This study combined theory and experiment to *tentatively* assign vibrational motions corresponding to

a HCH bend (1246 cm^{-1}), and CH symmetric (3121 cm^{-1}) and asymmetric (2854 cm^{-1}, 3237 cm^{-1}) stretches [63].

The most ground-breaking study of protonated methane was conducted by Asvany et al. in 2015. Here the authors used action spectroscopy methods to investigate trapped CH_5^+ at two different temperatures. At a temperature of 10 K, 2897 lines were observed from 2886−3116 cm^{-1} while 185 lines were observed at a temperature of 4 K. By constructing a combination difference coincidence spectrum the authors were able to isolate and assign individual lines of CH_5^+ [60]. In the event that some of the rotational assignments determined by this work turn out to be erroneous, Oka stresses that the combination differences obtained will remain correct. It is these combination differences that are the key to unraveling the mysteries of protonated methane, and the work of Asvany et al. is cited as putting experiment years ahead of theory in deciphering CH_5^+ [62].

The highly fluxional nature of CH_5^+ requires that high-level interactions be included in *ab initio* calculations in order to generate accurate results, posing a formidable challenge to theorists [64]. The potential energy surface (PES) of protonated methane has been calculated to have 120 equivalent global minima (corresponding to indistinguishable states of the five equivalent protons), all separated from each other by remarkably small barriers [60]. Despite even the best efforts, it is surmised that recent and continued experimental findings will enable the interstellar discovery of CH_5^+ long before a theoretical understanding of this ion can be achieved [62].

In the McCall lab, CH_5^+ could be investigated at multiple vibrational modes through the use of both the QCL and OPO. With a sensitive enough CRDS setup, or perhaps an 8.6 μm implementation of NICE-OHMS or NICE-OHVMS, it would be possible to investigate the CH bend frequency of CH_5^+ at 1250 cm^{-1} [50]. If necessary, high repetition-rate CRDS may be used to improve the sensitivity of the QCL spectrometer. With this method the sensitivity of CRDS may be improved by keeping the laser on resonance with the cavity and allowing for the more frequent acquisition of ringdowns. Regardless of the spectroscopic

method used, the frequency coverage of the QCL offers the basis for an instrument primely situated for investigation of the low-frequency bending motion of CH_5^+. Additionally, the frequency coverage of the OPO allows for the investigation of the perceived CH stretching modes of protonated methane using NICE-OHVMS.

$C_2H_4^+$

The ethylene cation is the simplest alkene cation, with one electron occupying a π bonding orbital in its ground electronic state [65]. Unlike neutral ethylene, ground state $C_2H_4^+$ has been shown to have a nonplanar structure that is twisted around the carbon-carbon bond [66]. Thus, this ion is believed to have torsional motion with calculations of the torsional angle having reported values varying from $14-33$ degrees [65]. This twisting motion is expected to lie very close to 84 cm^{-1} and the nonplanarity of $C_2H_4^+$ results in a classification of D_2 symmetry for this ion [67].

Infrared studies of the ethylene cation are largely rooted in photoelectron spectroscopy of both gaseous and solid-matrix deposited samples. An IR-vacuum ultraviolet pulsed field ionization-photoelectron method was used by Xing et al. in 2006 to verify the ν_1 to ν_{12} bands of $C_2H_4^+$ with some success [68]. A study by Chen et al. in 2015 confirmed a number of these bands in addition to providing low-resolution studies of several combination bands [65]. Table 3.2 summarizes the current state of knowledge of the mid-IR vibrational bands of this cation. While these studies provide enough information to enable investigations of these bands and occasionally yield partial rotational resolution, studies of $C_2H_4^+$ have yet to be performed at high-precision in the gas-phase.

$C_2H_5^+$

The ethyl cation, $C_2H_5^+$, represents the simplest alkene that can be formed through protonation of a double bond. $C_2H_5^+$ has been used as a theoretical testbed for *ab initio* methods, and is of particular interest due to the similar energies of its classical and non-classical structures. Extensive theoretical investigations have established the non-classical bridged-proton structure of $C_2H_5^+$ as the global minimum on the PES [59, 69]. Furthermore,

the classical $H_3C{-}CH_2^+$ structure is predicted to be only a saddle point which the non-classical structure traverses during the proton shift [59].

Experimental investigations have been conducted using IR photodissociation (IRPD) spectroscopy of $C_2H_5^+{-}Ar$ [70], $C_2H_5^+{-}Ar_2$ [70], and $C_2H_5^+{-}N_2$ [71]. These studies have confirmed the absence of a CH stretching band from 2800−2900 cm^{-1}, which provides evidence that the sp^3 moiety of a classical $H_3C{-}CH_2^+$ conformer is not present in the gas phase. Vibrational bands above 3000 cm^{-1} consistent with the non-classical structure were also detected in these studies, and IRPD has provided direct evidence of the bridged-proton stretch near 2158 cm^{-1} [70]. The previous work has been successful in confirming non-classical $C_2H_5^+$ as the stable conformer in the gas phase, but the presence of Ar/N_2 necessary to enable IRPD affects the observed band center. In addition, the lack of resolved rotational structure make these studies ineffective for guiding astronomical searches.

$C_2H_6^+$

While $C_2H_4^+$ and $C_2H_5^+$ remain largely uninvestigated at high-resolution, experimental studies exist to help guide future gas-phase studies of these ions. $C_2H_6^+$, on the other hand, has never been observed experimentally. As of this writing, the only study that exists to guide future investigations of this ion is found in the work of Kurosaki and Takayanagi where vibrational frequencies are calculated from the expected equilibrium geometry of $C_2H_6^+$ [72]. The accuracy of these frequencies should be noted with caution as the *ab initio* methods of the 1990s were not as developed as the methods available today. A collaboration with theoreticians is likely necessary to facilitate a high-resolution investigation of $C_2H_6^+$.

$C_2H_7^+$

Protonated ethane ($C_2H_7^+$) is the key intermediate in the reaction of CH_4 with CH_3^+ to form $C_2H_5^+$ [73]. Additionally, like $C_2H_3^+$ and $C_2H_5^+$, $C_2H_7^+$ is most stable in its non-classical form with the two carbon atoms and one hydrogen atom participating in a three-center, two-electron bond. Using a two-color laser scheme to probe mass-selected ions in a radio-frequency octopole ion trap, Yeh et al. observed what they deduced to be *both* the classical

and non-classical forms of $C_2H_7^+$ using an expansion discharge [12]. This deduction followed from the strong dependence of the obtained spectrum on the backing pressure and ratio of hydrogen to ethane used. In this work, the more stable structure was reasoned to not depend on the source backing pressure, and the experimentally obtained vibrational frequencies of this non-classical conformer are reported in Table 3.2 [12].

Ion	**Frequency (cm^{-1})**	**Notes**
CH_5^+	1246 [63]	
	2854 [63]	
	3121 [63]	
	3237 [63]	
$C_2H_4^+$	2873 [68]	ν_{11}, 68 km/mol
	2979 [68]	ν_2+ν_{12} combination band
$C_2H_5^+$	2996 [71]	b_2 symmetry, CH symmetric stretch, 34 km/mol
	3117 [71]	b_1 symmetry, CH asymmetric stretch, 70 km/mol
$C_2H_7^+$	2945 [12]	ν_6, symmetric CH stretch out of phase
	3082 [12]	ν_4, asymmetric CH stretch out of phase
	3128 [12]	ν_2, asymmetric CH stretch in phase

Table 3.2: Carbon-ion vibrational frequencies within the range of the OPO and QCL laser systems.

3.3 Nitrogen-Only Ions

Simple molecular ions comprised of nitrogen have long been a focus of spectroscopic investigations. NH_2^+, NH_3^+, and NH_4^+ have all been analyzed by high-resolution techniques, allowing the structure and dynamics of these species to be well-characterized (See [74–77] and references therein). Likewise, protonated nitrogen has been the focus of many studies due to its importance in laboratory discharge plasmas and the ISM [24]. The ν_1, ν_2, and ν_3 fundamental bands of HN_2^+ have been studied at high-resolution using diode laser and

velocity-modulated color-center laser spectrometers [78–81]. Protonated nitrogen was also the first ion to be studied by infrared-microwave double resonance spectroscopy [82, 83].

Interestingly, the spectrum of HN_2^+ was discovered in the ISM prior to any laboratory microwave or infrared studies were conducted [84]. In the same issue of *The Astrophysical Journal*, the unidentified triplet of lines at 93.174 GHz was tentatively assigned to HN_2^+ based on self-consistent field calculations of the rotational constant and hyperfine structure of this ion [85]. This assignment was quickly confirmed by Thaddeus and Turner in 1975 through further resolution of the hyperfine structure of the nitrogen nucleus [86]. Following this confirmation, a laboratory microwave study of HN_2^+ provided an additional check of these astronomical measurements [87].

Despite their hypothesized importance to interstellar and terrestrial chemical processes, studies of more complex nitrogen-containing ions remain scarce. *Ab initio* theoretical investigations and low-resolution photoelectron spectroscopy studies constitute much of the work that has been done on these ions, and provide a basis for future high-resolution studies as highlighted in the subsequent paragraphs.

$N_2H_2^+$

The diazene cation, $N_2H_2^+$, is important to the atmospheric chemistry of Jupiter's moon, Titan, and is believed to be an important component of biological nitrogen fixation [88]. Similar to $O_2H_2^+$, the diazene cation is expected to be most stable in its planar *trans*-$HNNH^+$ form [89, 90]. Isomerization between *trans*-$HNNH^+$ and the next most stable conformer, isodiazene (H_2NN^+), requires an energy of 54.0 kcal/mol to facilitate the transfer of an H-atom between the heavy atoms [90]. The other local minimum present on the $N_2H_2^+$ PES corresponds to the *cis*-$HNNH^+$ isomer, which exists slightly higher in energy than the isodiazene cation conformer.

The only experimental study of the diazene cation to date was performed by Frost et al. in 1976. Here, photoelectron spectroscopy of diazene (N_2H_2) was performed by introducing gas-phase pre-synthesized N_2H_2 (which necessarily contained small amounts of H_2 and N_2)

into the photoionization chamber. At the time of publication, this study resulted in the clear identification of a vibrational band near 1180 cm^{-1} [91]. A theoretical investigation performed in 2009 highlighted good agreement with the results of Frost et al. and further identifies additional bands that lie within the range of the OPO and QCL laser, which are summarized in Table 3.3 [92]. These previous studies provide ample information for initial high-resolution investigations of gas-phase *trans*-$HNNH^+$.

$N_2H_3^+$

Organic derivatives of diazene (N_2H_2) and hydrazine (N_2H_4) are of interest as potential hydrogen storage systems, and it follows that investigations into their protonated counterparts may offer insight into the mechanisms involved with such systems [93]. Although it remains uninvestigated experimentally, protonated diazene ($N_2H_3^+$) has been the subject of several theoretical studies that may help to guide a high-resolution study of this ion. The global minimum on the PES corresponds to the singlet-state, $H_2N_2H^+$ planar structure that is highly stable [90]. A theoretical study performed by Matus et al. in 2006 highlights three bands within the coverage of lasers available in the lab near 1200, 3330, and 3473 cm^{-1}, but it should be noted that currently no experimental evidence exists to support these calculated band frequencies [93].

$N_2H_4^+$

Throughout the literature there is some controversy over whether $N_2H_4^+$ exists in a D_{2h} or C_{2h} symmetric structure. While a photoelectron spectroscopic study of hydrazine was conducted in the early 1970s this work provides structural information only about neutral hydrazine, and no spectroscopic parameters that could be used to guide a search for $N_2H_4^+$ [94]. Theoretical work done by Habas et al. in 1997 predicts vibrational frequencies for $N_2H_4^+$ in both the D_{2h} and C_{2h} form, with the calculated frequencies differing by only a few wavenumbers. The D_{2h} structure is calculated to have bands at 3484, 3506, and 3651 cm^{-1}, while the analogous bands of the C_{2h} structure are calculated to be at 3489, 3510, and 3644 cm^{-1}, respectively [95]. These predictions may be useful for guiding high-resolution studies

that could help to resolve the discrepancy over the exact structure of this ion.

$N_2H_5^+$

Like protonated diazene, protonated hydrazine ($N_2H_5^+$) may be of interest to hydrogen storage. An experimental study performed in 1952 marked the first observation of $N_2H_5^+$, showing vibrational bands at 1124 cm^{-1} and multiple bands in the range of 2716−3261 cm^{-1} [96]. A more recent *ab initio* study predicts a band near 1210 cm^{-1} and five bands in the region of 3355−3519 cm^{-1} [93]. While these new predicted frequencies differ quite significantly from those obtained in the first studies of $N_2H_5^+$, the work by Pearson et al. suffered from extremely low resolution. Therefore, in this instance it may be more beneficial to begin a high-resolution survey at the frequencies predicted by Matus et al. rather than those of early experimental work [93, 96].

Ion	**Frequency (cm^{-1})**	**Notes**
$N_2H_2^+$	1183.9 [90]	ν_3, symmetric HNN in-plane bending
	3080.1 [90]	ν_4, antisymmetric HN stretch
	3083.6 [90]	ν_1, symmetric HN stretch
$N_2H_3^+$	1200 [93]	Theoretical prediction
	3330 [93]	Theoretical prediction
	3473 [93]	Theoretical prediction
$N_2H_4^+$	3483/3489 [95]	
	3506/3510 [95]	
	3651/3644 [95]	
$N_2H_5^+$	1210 [93]	
	3355−3519 [93]	5 bands predicted within this range

Table 3.3: Vibrational frequencies of nitrogen-only ions. For $N_2H_4^+$, all reported frequencies are theoretically predicted and are reported in a D_{2h}/C_{2h} format.

3.4 Oxygen-Only Ions and Ionized Water Clusters

Oxygen-containing molecular ions play a role in atmospheric chemistry, combustion, plasma chemistry, and biological processes [97, 98]. To this day several ions containing two oxygen atoms, including the elusive O_2H^+ ion and $O_2H_2^+$, remain uninvestigated experimentally. Moving to two-oxygen species of increasing complexity, $O_2H_4^+$ represents the simplest ion that can be formed from ionization of a water cluster (namely from the removal of an electron from the water dimer, $(H_2O)_2$). As the composition of cationic water cluster systems increases ($O_2H_5^+$, $O_2H_6^+$, etc.), the theoretical methods necessary to successfully model these systems drastically rise in complexity. The successful experimental observation of these species would provide the data necessary to guide future *ab initio* studies of charged water cluster systems.

A better understanding of water clusters is of great importance to the scientific community due to water's existence as one of the most prevalent polar solvents and the importance of water clusters to atmospheric chemistry [99]. Hydroxyl radicals produced upon ionization of neutral water clusters are associated with damage of living cells [100]. Studies have been conducted to investigate ionized water clusters, electron attachment and localization in neutral water clusters, and the fragmentation patterns that occur upon ionization of neutral water clusters [99].

Ionized water clusters can be largely divided into two classes: protonated $(H_2O)_nH^+$ and unprotonated $(H_2O)_n^+$. Despite experimental efforts, the structures of unprotonated ionized water clusters remain largely unknown due to the fact that these clusters are formed in highly vibrationally excited states that quickly lead to dissociation [99]. Investigations of unprotonated water clusters at high-resolution may require the use of a supersonic expansion discharge to prolong the existence of these clusters for spectroscopic investigation. Here, a method of sample introduction similar to that used in gas-phase vacuum-UV photoionization and electron impact ionization studies by Shinohara et al. could be used to yield significant amounts of unprotonated water clusters [101]. A number of experimental and theoretical

studies have also focused on protonated water clusters as will be discussed for $(H_2O)_2H^+$, an ion of great importance to the chemistry of the upper atmosphere [99].

O_2H^+

Protonated oxygen is expected to play a part in many processes including the chemistry of combustion and H_2/O_2 plasmas [97]. In addition, this ion is thought to be important to atmospheric chemistry and biological respiration [98]. Despite its hypothesized ubiquity, O_2H^+ remains unobserved to this day. Several attempts to predict the ν_1 fundamental band of O_2H^+ have been made, with predicted frequencies starting near 3500 cm^{-1} and lowering as theoretical methods improve [102]. Utilizing a tagged IR predissociation spectroscopy study, Nizkorodov et al. predicts the vibrational frequency for the OH stretch of HO_2^+ to be at 3020 ± 40 cm^{-1} [103]. This lower predicted value may explain why an attempt to observe O_2H^+ by the Oka group in 1991 ($\sim$3250$-$3600 cm^{-1}) failed to detect this ion, and instead resulted in the acquisition of a spectrum of H_3O^+ [102].

$O_2H_2^+$

The hydrogen peroxide cation ($HOOH^+$) and the oxywater cation (H_2OO^+) are the two most stable conformers of the cation composed of two oxygen and two hydrogen atoms. $HOOH^+$ is calculated to be the most stable of the conformers, with H_2OO^+ existing as a local minimum +23 kcal/mol higher on the PES [89]. Isomerization between the two species requires an activation barrier of $\sim$33 kcal/mol be surmounted, and in doing so the planar $HOOH^+$ structure is transformed into the pyramidal shape of H_2OO^+. The $HOOH^+$ isomer may exist as either *cis* or *trans*-$HOOH^+$, with *trans* being the more stable planar structure by 8 kcal/mol [89].

These species have been formed successfully in the gas phase via ionization of gaseous mixtures of oxygen and water using chemical ionization. Here the ratio of $HOOH^+$ to H_2OO^+ was shown to be dependent on the composition of the precursor gas mixture [104]. Recently, Thompson et al. recorded the infrared spectrum of the *trans*-$HOOH^+$ isomer trapped in solid neon. In this study a moderately strong peak corresponding to the ν_5 vibration of

trans-$HOOH^+$ was observed near 3237.0 cm^{-1} [105]. While this band center is likely to be altered slightly from gas-phase *trans*-$HOOH^+$ due to the neon matrix, this work provides a starting point for a high-resolution investigation of this ion using OPO NICE-OHVMS.

$O_2H_4^+$

Under relatively high pressure conditions the water dimer, $(H_2O)_2$, is known to form in the gaseous phase. This structure is stabilized by a strong hydrogen bond that forms between the two water molecules [106]. Upon ionization the water dimer undergoes a significant geometric relaxation, as shown by a photoelectron spectroscopy study [107]. The ionized complex is expected to exhibit large amplitude motion as a result of a hydrogen atom being shared among the two oxygen centers, and is most accurately modeled by anharmonic methods [108].

A more recent study combined experiment with theory to unambiguously determine the structure of the most stable conformer of $O_2H_4^+$ as an ion-radical complex most easily expressed as $H_3O^+ - {}^{\bullet}OH$. This conclusion was drawn from IR transitions observed from 1000−4000 cm^{-1} in argon-tagged predissociation spectra acquired for $H_4O_2^+ - Ar$ and $H_4O_2^+ - Ar_2$ formed in a pulsed supersonic expansion photofragmentation spectrometer. Of particular note from this study is the observation of a band near 3392 cm^{-1}, which was observed to be independent of the number of argon atoms involved in the predissociation spectra, and could serve as a starting point in discovery spectroscopy of this ionic water cluster species [108].

$O_2H_5^+$

The protonated water dimer, $(H_2O)_2H^+$, is generally considered to be the prototypical system for the study of proton transfer in solution [110]. Proton mobility is of strong interest to biological and chemical processes, and protonated water clusters are noteworthy components of the upper atmosphere, with $(H_2O)_2H^+$ being the dominant ionized species present in the D region of the ionosphere [99, 110, 113]. $(H_2O)_2H^+$ is also of interest due to the exceedingly strong nature of the hydrogen bond that binds the central proton to the

Ion	Frequency (cm^{-1})	Notes
O_2H^+	3020 [103]	Theoretical prediction
$O_2H_2^+$	3237 [103]	*trans*-HOOH isomer
$O_2H_4^+$	3392 [108]	
$O_2H_5^+$	1163 [109]	Disputed, observed at 1252 cm^{-1} by work of Asmis et al. [110]
	3603 [111]	Agrees well with 3609 cm^{-1} of Yeh et al. [112]
	3683 [111]	Agrees well with 3684 cm^{-1} of Yeh et al. [112]

Table 3.4: Vibrational frequencies of oxygen-containing molecular ions.

two surrounding water molecules. While the typical strength of a hydrogen bond is 10−20 kJ/mol, the strength of the hydrogen bond associated with the protonated water dimer is 130 kJ/mol [109]. Both the cause and effects of this abnormally strong hydrogen bond may be better understood through a thorough investigation into the structure and behavior of this system.

With its prevalent role in proton transfer in aqueous solution, $O_2H_5^+$ has been studied by theoretical methods for more than 30 years. However, these theoretical studies are made difficult due to large amplitude motions that result from the flat nature of the PES near the global minimum and low-energy pathways for rearrangement [114]. A recent quantum Monte Carlo study utilizing highly correlated wave functions to investigate the minimum energy equilibrium structure confirms the Zundel configuration as the minimum energy structure [115]. The Zundel cation is best described as two water molecules bound by an evenly-shared central proton, giving the structure C_2 symmetry. This finding agrees well with previous theoretical studies and exhibits an accuracy comparable to more expensive coupled cluster theory methods, which demonstrates the ubiquity of $O_2H_5^+$ as a test system for improving the efficacy of *ab initio* methods for complex systems [115].

Gas-phase experimental spectra of the $(H_2O)_2H^+$ structure exist to guide theory, but many of these studies have been done at low-resolution or are missing crucial information necessary to fully characterize this system. In 1989, Yeh at al. used two-color infrared multi-

photon dissociation spectroscopy of a corona discharge source to obtain low-resolution (0.5 cm^{-1}) spectra of $O_2H_5^+$ from 3550−3880 cm^{-1}, identifying two OH stretching bands near 3609 cm^{-1} (symmetric) and 3684 cm^{-1} (antisymmetric) [112]. Modifications to the laser scheme then allowed for a high-resolution (0.01 cm^{-1}) study of the antisymmetric stretch near 3700 cm^{-1} in 1994, revealing spectral splittings due to tunneling motion [116]. However, in this study water absorption of the laser radiation precluded a complete study of the Q-branch of this ion and further studies into this region are necessary to fully characterize the extent of the perceived tunneling effects involved with $(H_2O)_2H^+$ [116]. It should be noted that a theoretical study by Vendrell et al. in 2007 further confirmed the presence of vibrational bands at 3603 cm^{-1} and 3683 cm^{-1}, in good agreement with the experimental observations of Yeh and coworkers in 1989 and 1994 [111, 112, 116].

Lower-frequency (600−1900 cm^{-1}) gas-phase and theoretical studies done in 2003 and 2004 investigated the vibration associated with the proton shared between the two water molecules in $(H_2O)_2H^+$ [109,110,114]. Asmis et al. utilized a tandem mass spectrometer−ion trap apparatus in combination with a free electron laser to elucidate a shared-proton vibration near 1252 cm^{-1} [110]. However, in 2004 an experimental study performed by Fridgen et al. identified this same band as having a characteristic frequency of 1163 cm^{-1} [109]. The discrepancy between these results is still not fully resolved, but future experimental investigations into this band using the QCL may be monumental in characterizing this region and providing essential benchmarks for theoretical investigations of the shared-proton vibration of $(H_2O)_2H^+$ [109].

Beyond the Zundel cation, investigations into deuterated versions of this ion as well as larger protonated water clusters will generate insight into proton transfer in solution, among other processes. For deuterated versions of the protonated water dimer, the work of Agostini et al. provides extensive theoretical information as to where high-resolution experimental studies may begin [117]. Additionally, low-resolution experimental studies of $O_3H_7^+$ and $O_4H_9^+$ provide a springboard for the experimentalist looking to fully resolve the

role of tunneling and hydrogen-bonding in protonated water clusters [112,116]. It should be noted that the aforementioned studies show that both of these cluster species are known to have OH stretching modes within the coverage of the OPO (near 3700 cm^{-1}).

3.5 Carbon-Nitrogen Ions

Regarding molecular ions consisting of carbon and nitrogen, protonated hydrogen cyanide ($HCNH^+$) has attracted much attention due to its importance in interstellar chemistry as the main precursor to HCN and HNC molecules in interstellar space. Thanks to millimeter-wave spectroscopic investigations of this ion, rotational transitions have been determined that have enabled the detection of $HCNH^+$ in the ISM (in the direction of Sgr B2) [118,119]. Additionally, $\nu_1 - \nu_5$ have been investigated using high-resolution spectroscopy and high-level *ab initio* methods [120–126]. Despite their expected prevalence in interstellar chemistry and physical processes occurring here on Earth, several carbon-nitrogen ions have yet to be investigated by high-resolution spectroscopy as discussed in more detail below.

HCN^+ and HNC^+

Neutral hydrogen cyanide (HCN) and hydrogen isocyanide (HNC) have been widely studied due to their importance in various chemical systems and their presence in dense interstellar clouds [127]. These studies have led to the determination that HCN is more stable than HNC by 42−50 kJ/mol, with HNC existing as a metastable isomer. In contrast, the hydrogen cyanide cation (HCN^+) is predicted to be less stable than the hydrogen isocyanide cation (HNC^+), with the two systems having very different chemical reactivities [128]. FT-IR absorption spectroscopy of HCN deposited in solid neon passed through a microwave discharge confirms the existence of both HCN^+ and HNC^+, and has established vibrational frequencies in good agreement with those determined for gas-phase ionized HCN and HNC. Specifically, HCN^+ has been experimentally determined to have a ν_1 (CH stretch) vibration at 3050 cm^{-1}, HNC^+ at 3365 cm^{-1}, DCN^+ at 2374 cm^{-1}, and DNC^+ at 2664 cm^{-1} [128].

As shown in Table 3.5, *ab initio* predictions of the vibrational bands of these ions differ significantly for all but the 3465 cm^{-1} band of HNC^+ [127]. Further experimental study of the isomers and isotopologues of HCN^+ are needed to resolve these discrepancies.

H_2CN^+

The singlet state $HCNH^+$ isomer of protonated hydrogen cyanide has been proven by many theoretical and experimental methods to exist as the sole global minimum on the PES of this ion, and this isomer has been widely studied as noted in the introduction [125,126,129]. The triplet-state H_2CN^+ isomer is predicted to exist as a local minimum on the PES of the $[H_2,C,N]^+$ ion and may be observable experimentally [129, 130]. However, this mode is believed to lie at 1299 cm^{-1}, and may be just outside of the range currently accessible to the QCL [129].

Ion	**Frequency (cm^{-1})**
HCN^+	3050 (3099)
DCN^+	2374 (2416)
HNC^+	3365 (3464)
DNC^+	2665 (2727)
H_2CN^+	1299 [129]

Table 3.5: Carbon-Nitrogen molecular ion vibrational frequencies. For those ions with two frequencies listed, experimentally observed frequencies by Forney et al. [128] are listed first with theoretically predicted frequencies by Peterson et al. [127] given in parentheses.

$[C,N,H_3]^+$, $[C,N,H_4]^+$

As the number of hydrogen atoms attached to CN increases, the exact structure of carbon-nitrogen containing ions becomes more difficult to determine. This is evidenced by the lack of *ab initio* and experimental data for the $[C,N,H_3]^+$ and $[C,N,H_4]^+$ molecular ions. Since the mid-1990s there has been debate over the structure of the $[C,N,H_3]^+$ ion, with the $HCNH_2^+$ and H_2CNH^+ isomers alternately cited as the global minimum on the PES [131, 132]. In both of these studies it should be noted that the energy difference between the two minima was very small (∼10 kcal/mol) [131, 132]. To this day no experimental or theoretical studies

of this ion exist, and a collaboration with theorists will be necessary to guide a search for this ion.

3.6 Carbon-Oxygen Ions

With its large dipole moment of >4 Debye, the formyl cation (HCO+) exhibits strong rotational transitions that enabled its discovery in the interstellar medium years before its laboratory characterization [133]. In 1970 Buhl and Snyder discovered an unidentified line at 89.190 GHz while searching for hydrogen cyanide [134]. At the time it was speculated that this line belonged to HCO+, but this assignment was not confirmed until a laboratory study performed by Woods et al. five years later [135, 136]. HCO^+ was also the first ion to be studied by velocity-modulation spectroscopy, and has been extensively characterized by various spectroscopic techniques [7]. The molecular structure of HCO^+ was first determined in 1981 through measurements of the J=0→1 rotational transition of this ion and its isotopically substituted variants [137]. Studies using difference-frequency and diode lasers quickly followed, resolving numerous lines within the IR-active ν_1 and ν_3 fundamental bands [133, 138, 139]. In 2007, Lattanzi et al. extended the work done on HCO^+ to the terahertz regime to provide coverage of frequencies accessible to the Herschel Space Observatory and the Atacama Large Millimeter Array (ALMA) [140]. Additionally, indirect rotational spectroscopy was performed on this ion in 2013 to determine the rotational spectrum up to J=10←9 in the ν_1 first excited state [7].

As a precursor to one of the most abundant interstellar molecules (formaldehyde), the more complex H_3CO^+ ion has been the subject of numerous theoretical and experimental studies [141]. While early theoretical methods predicted H_3CO^+ to be the most stable form of this ion, more recent calculations revealed H_2COH^+ to be the most stable isomer [141,142]. Experimentally, H_2COH^+ was first detected through its OH stretch near 2.9 μm by Amano and Warner in 1989, and rotational spectroscopy of this ion quickly followed [141, 143, 144].

These studies enabled the detection of protonated formaldehyde towards SgrB2, OrionKL, and W51 in 1996, and helped to better characterize the fractional abundance of this ion in the ISM [145]. Although much work has already been done regarding H_2COH^+, studies continue to emerge that offer new insight into further characterization of this ion [142]. In addition, the primary ion formed from formaldehyde (H_2CO^+) is also hypothesized to be of importance to interstellar chemistry, but has not yet been studied at high-resolution [146].

Ion	**Frequency (cm^{-1})**[a]	**Notes**
H_2CO^+	1210.2 [147]	ν_3
	2580.2 [147]	ν_1, 170 km/mol
CH_3O^+	2469(2367) [142]	CH Stretch, 1028 km/mol
	2717(2626) [142]	Symmetric CH_2 stretch, 181.6 km/mol
	2747(2649) [142]	Asymmetric CH_2 stretch, 120.2 km/mol
H_2COH^+	2967(2977) [142]	Symmetric CH_2 stretch, 0.9 km/mol
	3124(3111) [142]	Asymmetric CH_2 stretch, 8.9 km/mol
	3182(3168) [142]	OH Stretch, 3423 cm^{-1} reported by Amano and Warner [141]

Table 3.6: Vibrational frequencies of the formaldehyde cation and isomers of protonated formaldehyde. For CH_3O^+ and H_2COH^+, experimentally determined frequencies (Ar-tagged) are listed first, with theoretical predictions given in parentheses.

H_2CO^+

The primary ion formed as a result of the ionization of formaldehyde remains uninvestigated at high-resolution to this day, but several theoretical and photoelectron spectroscopy studies exist to guide a study of this ion. A theoretical study done by Sears et al. in 2008 highlights two minima on the PES that lie within 6 kcal/mol of each other. The global minimum was found to be the formaldehyde cation form (H_2CO^+), with *trans*-$HCOH^+$ existing at a slightly higher energy. No minimum corresponding to a *cis*-$HCOH^+$ isomer was found, providing evidence that only two stable conformers of this molecular ion exist [90].

Photoelectron spectroscopy of formaldehyde entrained in supersonic expansions have confirmed the infrared spectrum of H_2CO^+ contains a strong CH stretching mode near

2580.2 cm^{-1}, corresponding to the ν_1 vibration [147, 148]. Additionally, ν_3 near 1210.2 cm^{-1} has also been observed and may be a good target for future investigations using the QCL [147]. A method of sample introduction can be gleaned from that used to form gaseous formaldehyde for the study of H_2COH^+ using a difference frequency laser by Amano and Warner in 1989. This study utilized a mixture of hydrogen gas (∼1 torr) and H_2CO (formed by heating paraformaldehyde powder, ∼10 mTorr) in a hollow cathode discharge cell to observe protonated formaldehyde [141]. While this method of sample introduction may work well for plasma discharge cells, such as Black Widow, in the event that a supersonic expansion discharge is used other means of sample introduction have also been realized [147, 149, 150].

H_2COH^+ and H_3CO^+

While protonated formaldehyde has been detected in the ISM, there is still much to be learned about this ion through high-resolution spectroscopy of its IR-active fundamental bands [145]. H_2COH^+ has been confirmed as the most stable form of this ion, but further work has elucidated the potential presence of the H_3CO^+ isomer as a metastable species that should be experimentally observable [142]. A thorough analysis of the $[H_3,C,O]^+$ ion PES confirmed the H_2COH^+ conformer as the most stable structure [142]. This analysis also highlighted the existence of the H_3CO^+ isomer as a metastable species +96 kcal/mol higher in energy than H_2COH^+, and shows the $HCOH_2^+$ structure as a high-energy local minimum as well (although there is no experimental evidence to support the existence of this isomer) [142].

Experimental evidence of the methoxy cation (H_3CO^+) has been tentatively obtained through low-resolution IR laser photodissociation spectroscopy of ions expanded in a molecular beam. Further investigation of the experimentally observed bands near 2469, 2717, and 2747 cm^{-1} would provide more insight on the behavior of the methoxy cation, and would allow theorists to better characterize the PES of the $[H_3,C,O]^+$ ion. Likewise, while the OH stretch of the H_2COH^+ isomer has been well-characterized at high-resolution, analysis of the bands near 2967, 3124, and 3182 cm^{-1} would provide further benchmarks for theory. It

should be noted that all of the cited frequencies were obtained by Argon-tagged photodissociation spectroscopy and may be altered from tag-free gas-phase studies (as Argon binding location has been demonstrated to affect the frequencies of the CH and OH stretches of this system) [142].

3.7 Nitrogen-Oxygen Ions

Molecules consisting of nitrogen and oxygen are known to play important roles in combustion, atmospheric chemistry, and in processes that occur in the ISM [151–153]. Despite their pervasive importance, studies of both neutral and ionic nitrogen-oxygen containing systems remain scarce. The experimental literature that exists for these species largely derives information about their molecular structure from photoelectron spectroscopy [152]. As is the case for many systems that have yet to be thoroughly investigated in the laboratory, theoretical studies exist to guide future high-resolution studies of these ions as detailed below [153–155]. The very limited amount of information available for nitrogen-oxygen containing ions highlights a substantial gap in the literature that may be addressed through future work using NICE-OHVMS or a QCL spectrometer.

HNO^+ and HON^+

Nitroxyl (HNO) is known to be an important intermediate in the combustion of mixtures containing NH_3, NO, and O_2 [152]. In addition, neutral HNO has successfully been detected in the ISM [151]. The $[H,N,O]^+$ ion has been characterized using a multi-reference configuration-interaction (MRCI) approach and supports the existence of both HNO^+ and HON^+ isomers [153]. Both of these isomers are known to have a bent geometry in their ground state. HNO^+ is the lowest energy isomer, with a barrier to isomerization of nearly 20,000 cm^{-1} standing in the way of transfiguration to the HON^+ form [153]. This work further details HNO^+ as having a vibrational band near 2900 cm^{-1}, while HON^+ is calculated to have two bands within the coverage of lasers in the lab ($\sim$1170 and 3140 cm^{-1}) [153]. The

experimentally confirmed existence of a band near 2900 cm^{-1} for HNO^+ agrees well with a theoretical study done by Bruna et al. substantiating this frequency as a place to start when pursuing a spectroscopic investigation of this ion [156].

$[H_2,N,O]^+$ Ions

H_2NO is suspected of being involved in the catalytic destruction of ozone in the stratosphere [152]. The PES of the $[H_2,N,O]^+$ ion supports the existence of four isomers: H_2NO^+, *trans*-$HNOH^+$, *cis*-$HNOH^+$, NOH_2^+ (listed in order of increasing energy) [154,155]. The least stable NOH_2^+ isomer is known to form from mixtures of N_2/H_2O subjected to electron impact ionization, while H_2NO^+ may be formed by protonation of HNO using H_3O^+/CH_5^+ [154]. Photoelectron spectroscopy has been used to investigate H_2NO^+ and D_2NO^+, with D_2NO^+ tentatively possessing a vibrational band (ND_2 bending mode) within the coverage of the QCL at 1245 cm^{-1} [152].

Ion	**Frequency (cm^{-1})**	**Notes**
HNO^+	∼2900 [153]	NH stretching mode
HON^+	1170 [153]	Bending mode
	3140 [153]	NH stretching mode
D_2NO^+	1245 [152]	Experimentally observed D_2N bending mode

Table 3.7: Vibrational frequencies of nitrogen-oxygen containing molecular ions. Unless specifically noted, listed frequencies are theoretical values.

Appendix A

Calculation of the Saturation Parameter of OPO cm-NICE-OHMS

Details of the calculation of the saturation parameter (G) associated with the OPO cm-NICE-OHMS work are presented here, based on equations presented in Ma et al. [28].

With a coupling efficiency of ∼10%, approximately 50 mW of the ∼500 mW of the incident laser power enters the cavity. Based on the current cavity parameters, this translates to light with an intensity of ∼1.02 W/mm^2 circulating in the cavity. To calculate the saturation parameter, one must consider the amount of power present in the sidebands of the modulated light. Given a modulation index of ∼0.6, the intensity present in the sidebands is ∼0.08 W/mm^2, calculated using equations presented in Section 4.9 of the work of A. A. Mills [157]. It is then possible to calculate the saturation parameter for NICE-OHMS based on the following equation [28]:

$$G = \frac{2\mu^2 I}{3c\epsilon_0 \hbar^2 \gamma_{tt}^2} \tag{A.1}$$

Useful constants and conversions include: 1 D^2 = 10^{-36} erg×cm^3 and $\hbar = 1.055 \times 10^{-27}$ erg×s. For a dipole moment of ∼0.2 D, a relaxation rate dictated by the transit time of ions through the beam of ∼3 MHz, and an intensity of ∼0.08 W/mm^2, an upper limit to the saturation parameter is calculated to be ∼6 for J = 0. This value will be lower for higher J values, as the dipole moment of each transition is calculated by:

$$\mu_J = \mu \frac{J+1}{2J+1} \tag{A.2}$$

For comparison to the work of Ma et al. it is important to also determine a value:

$$y = \sqrt{\ln(2)} \times \frac{\gamma_{tt}}{\delta\nu_D} \tag{A.3}$$

In the Doppler limit ($y = 0$), only the intensity of absorption is affected by saturation. For OPO cm-NICE-OHMS the expected y-value is ∼0.01. At this value of y, absorption is only slightly affected by saturation ($< 5\%$ intensity change for G $\leq$ 10), and the dispersion intensity is virtually unaffected ($< 2\%$ intensity change for G $\leq$ 10). Even in the limit of extremely strong saturation (G = 100), saturation effects would only affect the dispersion intensity by a maximum of ∼7 % [28].

References

[1] N. M. Semo and W. S. Koski. Some ion-molecule reactions pertinent to combustion. *The Journal of Physical Chemistry*, 88:5320, 1984.

[2] R. D. Thomas. When electrons meet molecular ions and what happens next: Dissociative recombination from interstellar molecular clouds to internal combustion engines. *Mass Spectrometry Reviews*, 27(5):485, 2008.

[3] F. Cacace and G. de Petris. Mass spectrometric study of simple main group molecules and ions important in atmospheric processes. *International Journal of Mass Spectrometry*, 194:1, 2000.

[4] E. Herbst and W. Klemperer. The formation and depletion of molecules in dense interstellar clouds. *The Astrophysical Journal*, 185:505, 1973.

[5] D. Smith. The ion chemistry of interstellar clouds. *Chemical Reviews*, 92:1473, 1992.

[6] P. F. Bernath. *Spectra of atoms and molecules*. Oxford University Press.

[7] B. M. Siller, J. N. Hodges, A. J. Perry, and B. J. McCall. Indirect rotational spectroscopy of HCO^+. *The Journal of Physical Chemistry A*, 117:10034, 2013.

[8] T. Amano. Difference-frequency laser spectroscopy of molecular ions with a hollow-cathode cell: extended analysis of the ν_1 band of H_2D^+. *Journal of the Optical Society of America B*, 2:790, 1985.

[9] K. N. Crabtree, C. A. Kauffman, B. A. Tom, E. Beçka, B. A. McGuire, and B. J. McCall. Nuclear spin dependence of the reaction of H_3^+ with H_2 II. Experimental measurements. *The Journal of Chemical Physics*, 134:194311, 2011.

[10] K. N. Crabtree, J. N. Hodges, B. M. Siller, A. J. Perry, J. E. Kelly, P. A. Jenkins, and B. J. McCall. Sub-Doppler mid-infrared spectroscopy of molecular ions. *Chemical Physics Letters*, 551:1, 2012.

[11] P. C. Engelking. Corona excited supersonic expansion. *Review of Scientific Instruments*, 57:2274, 1986.

[12] L. I. Yeh, J. M. Price, and Y. T. Lee. Infrared spectroscopy of the pentacoordinated carbonium ion $C_2H_7^+$. *Journal of American Chemical Society*, 111:5597, 1989.

[13] Y. Xu, M. Fukushima, T. Amano, and A. R. W. McKellar. Infrared absorption spectroscopy of molecular ions in a corona-discharge slit expansion. *Chemical Physics Letters*, 242:126, 1995.

[14] D. T. Anderson, S. Davis, T. S. Zwier, and D. J. Nesbitt. An intense slit discharge source of jet-cooled molecular ions and radicals ($T_{rot} < 30K$). *Chemical Physics Letters*, 258:207, 1996.

[15] S. Davis, M. Fárník, D. Uy, and D. J. Nesbitt. Concentration modulation spectroscopy with a pulsed slit supersonic discharge expansion source. *Chemical Physics Letters*, 344:23, 2001.

[16] K. N. Crabtree, C. A. Kauffman, and B. J. McCall. A modular and robust continuous supersonic expansion discharge source. *Review of Scientific Instruments*, 81:86103, 2010.

[17] T. Nakanaga, F. Ito, K. Sugawara, H. Takeo, and C. Matsumura. Observation of infrared absorption spectra of molecular ions, H_3^+ and HN_2^+, by FTIR spectroscopy. *Chemical Physics Letters*, 169:269, 1990.

[18] C. M. Western. PGopher, A program for simulating rotational, vibrational and electronic structure. *University of Bristol*, http://pgopher.chm.bris.ac.uk.

[19] A. Foltynowicz, F. Schmidt, W. Ma, and O. Axner. Noise-immune cavity-enhanced optical heterodyne molecular spectroscopy: Current status and future potential. *Applied Physics B*, 92:313, 2008.

[20] J. Ye, L. Ma, and J. L. Hall. Ultrasensitive detections in atomic and molecular physics: demonstration in molecular overtone spectroscopy. *Journal of the Optical Society of America B*, 15:6, 1998.

[21] B. M. Siller, M. W. Porambo, A. A. Mills, and B. J. McCall. Noise immune cavity enhanced optical heterodyne velocity modulation spectroscopy. *Optics Express*, 19:24822, 2011.

[22] M. W. Porambo, B. M. Siller, J. M. Pearson, and B. J. McCall. Broadly tunable mid-infrared noise-immune cavity-enhanced optical heterodyne molecular spectrometer. *Optics Letters*, 37:4422, 2012.

[23] C. M. Lindsay and B. J. McCall. Comprehensive evaluation and compilation of H_3^+ spectroscopy. *Journal of Molecular Spectroscopy*, 210:60, 2001.

[24] Y. Kabbadj, T. R. Huet, B. D. Rehfuss, C. M. Gabrys, and T. Oka. Infrared spectroscopy of highly excited vibrational levels of protonated nitrogen, HN_2^+. *Journal of Molecular Spectroscopy*, 163:180, 1994.

[25] M. W. Porambo. *Development of a sensitive mid-infrared spectrometer for the study of cooled molecular ions.* PhD thesis, The University of Illinois, 2015.

[26] C. H. Townes and A. L. Schawlow. *Microwave Spectroscopy.* McGraw-Hill, 1955.

[27] M. Louviot, N. Suas-David, V. Boudon, R. Georges, M. Rey, and S. Kassi. Strong thermal nonequilibrium in hypersonic CO and CH_4 probed by CRDS. *The Journal of Chemical Physics*, 142:214305, 2015.

[28] W. Ma, A. Foltynowicz, and O. Axner. Theoretical description of doppler-broadened noise-immune cavity-enhanced optical heterodyne molecular spectroscopy under optically saturated conditions. *The Journal of the Optical Society of America B*, 25:1144, 2008.

[29] F. Dong, D. Uy, S. Davis, M. Child, and D. J. Nesbitt. Supersonically cooled hydronium ions in a slit-jet discharge: High-resolution infrared spectroscopy and tunneling dynamics of HD_2O^+. *The Journal of Chemical Physics*, 122:224301, 2005.

[30] F. Dong and D. J. Nesbitt. Jet cooled spectroscopy of H_2DO^+: Barrier heights and isotope-dependent tunneling dynamics from H_3O^+ to D_3O^+. *The Journal of Chemical Physics*, 125:144311, 2006.

[31] D. Zhao, K. D. Doney, and H. Linnartz. Laboratory gas-phase detection of the cyclopropenyl cation (c-$C_3H_3^+$). *The Astrophysical Journal Letters*, 791:L28, 2014.

[32] A. J. Perry, J. N. Hodges, C. R. Markus, G. S. Kocheril, and B. J. McCall. Communication: High-precision sub-Doppler infrared spectroscopy of the HeH^+ ion. *The Journal of Chemical Physics*, 141:101101–1, 2014.

[33] A. J. Perry, J. N. Hodges, C. R. Markus, G. S. Kocheril, and B. J. McCall. High-precision R-branch transitions in the ν_2 fundamental band of H_3^+. *The Journal of Molecular Spectroscopy*, 317:71, 2015.

[34] C. R. Markus, J. N. Hodges, A. J. Perry, G. S. Kocheril, and H. S. P. M˙High precision rovibrational spectroscopy of OH^+.

[35] J. J. Thomson. Rays of positive electricity. *Philosophical Magazine*, 21:225, 1911.

[36] B. J. McCall and T. Oka. H_3^+- an ion with many talents. *Science*, 287:1941, 2000.

[37] T. Oka. Observation of the infrared spectrum of H_3^+. *Physical Review Letters*, 45:531, 1980.

[38] L. Trafton, D. F. Lester, and K. L. Thompson. Unidentified emission lines in Jupiter's northern and southern 2 micron aurorae. *The Astrophysical Journal*, 343:L73, 1989.

[39] M. Okumura, L. I. Yeh, and Y. T. Lee. The vibrational predissociation spectroscopy of hydrogen cluster ions. *The Journal of Chemical Physics*, 83:3705, 1985.

[40] P. Barragán, R. P. de Tudela, R. Prosmiti, P. Villarreal, and G. Delgado-Barrio. Path integral Monte Carlo studies of the H_5^+/D_5^+ clusters using *ab initio* potential surfaces. *Physica Scripta*, 84:28109, 2011.

[41] J. W. Young, T. C. Cheng, B. Bandyopadhyay, and M. A. Duncan. IR Photodissociation spectroscopy of H_7^+, H_9^+, and their deuterated analogues. *The Journal of Physical Chemistry A*, 117:6984, 2013.

[42] P. H. Dawson and A. W. Tickner. Detection of H_5^+ in the hydrogen glow discharge. *The Journal of Chemical Physics*, 37:672, 1962.

[43] Z. Lin and A. B. McCoy. The role of large-amplitude motions in the spectroscopy and dynamics of H_5^+. *The Journal of Chemical Physics*, 140:114305, 2014.

[44] T. C. Cheng, L. Jiang, K. R. Asmis, Y. Wang, J. M. Bowman, A. M. Ricks, and M. A. Duncan. Mid- and far-IR spectra of H_5^+ and D_5^+ compared to the predictions of anharmonic theory. *The Journal of Physical Chemistry Letters*, 3:3160, 2012.

[45] T. C. Cheng, B. Bandyopadyay, Y. Wang, S. Carter, B. J. Braams, J. M. Bowman, and M. A. Duncan. Shared-proton mode lights up the infrared spectrum of fluxional cations H_5^+ and D_5^+. *The Journal of Physical Chemistry Letters*, 1:758, 2010.

[46] Z. Lin and A. B. McCoy. Signatures of large-amplitude vibrations in the spectra of H_5^+ and D_5^+. *The Journal of Physical Chemistry Letters*, 3:3690, 2012.

[47] Y. Yamaguchi, J. F. Gaw, R. B. Remington, and H. F. Schaefer. The H_5^+ potential energy hypersurface: Characterization of ten distinct energetically low-lying stationary points. *The Journal of Chemical Physics*, 86:5072, 1987.

[48] Á. Valdés and R. Prosmiti. Theoretical investigation of the infrared spectra of the H_5^+ and D_5^+ cations. *The Journal of Physical Chemistry A*, 117:9518, 2013.

[49] B. A. McGuire, Y. Wang, J. M. Bowman, and S. L. W. Weaver. Do H_5^+ and its isotopologues have rotational spectra? *The Journal of Physical Chemistry Letters*, 2:1405, 2011.

[50] E. T. White, J. Tang, and T. Oka. CH_5^+: The infrared spectrum observed. *Science*, 284:135, 1999.

[51] M. R˙ Detection of the infrared spectrum of CH_2^+.

[52] M. F. Jagod, C. M. Gabrys, and M. R˙ Infrared spectrum of CH_3^+ involving high rovibrational levels.

[53] M. W. Crofton, M. F. Jagod, B. D. Rehfuss, W. A. Kreiner, and T. Oka. Infrared spectroscopy of carbo-ions. III. ν_3 band of methyl cation CH_3^+. *The Journal of Chemical Physics*, 88:667, 1988.

[54] R. Signorell and F. Merkt. The first rotationally resolved spectrum of CH_4^+. *The Journal of Chemical Physics*, 110:2309, 1999.

[55] M. W. Crofton, M. Jagod, B. D. Rehfuss, and T. Oka. Infrared spectroscopy of carboions. V. Classical vs nonclassical structure of protonated acetylene $C_2H_3^+$. *The Journal of Chemical Physics*, 91:5139, 1989.

[56] M. W. Crofton, M. Jagod, B. D. Rehfuss, and T. Oka. Infrared spectra of carboions. II. ν_3 band of acetylene ion $C_2H_2^+$ ($^2\pi_u$). *The Journal of Chemical Physics*, 86:3755, 1987.

[57] C. M. Gabrys, D. Uy, M. Jagod, T. Oka, and T. Amano. Infrared spectroscopy of carboions. 8. Hollow cathode spectroscopy of protonated acetylene, $C_2H_3^+$. *The Journal of Chemical Physics*, 99:15611, 1995.

[58] M. Jagod and M. R˙Infrared spectroscopy of carbo-ions. VI. C−H stretching vibration of the acetylene ion $C_2H_2^+$ and isotopic species.

[59] W. Quapp and D. Heidrich. Exploring the potential energy surface of the ethyl cation by new procedures. *Journal of Molecular Structure (Theochem)*, 585:105, 2002.

[60] O. Asvany, K. M. T. Yamada, and S. Br˙ Experimental ground-state combination differences of CH_5^+.

[61] O. Asvany, P. Kumar, B. Redlich, I. Hegemann, S. Schlemmer, and D. Marx. Understanding the infrared spectrum of bare CH_5^+. *Science*, 309:1219, 2005.

[62] T. Oka. Taming CH_5^+, the "enfant terrible" of chemical structures. *Science*, 347:1313, 2015.

[63] X. Huang, A. B. McCoy, J. M. Bowman, L. M. Johnson, C. Savage, F. Dong, and D. J. Nesbitt. Quantum deconstruction of the infrared spectrum of CH_5^+. *Science*, 311:5757, 2006.

[64] S. D. Ivanov, A. Witt, and D. Marx. Theoretical spectroscopy using molecular dynamics: Theory and application to CH_5^+ and its isotopologues. *Physical Chemistry Chemical Physics*, 15:10270, 2013.

[65] S. Chen, M. Liu, T. Huang, C. Chin, and Y. Wu. Photodissociation and infrared spectra of ethylene cations in solid argon. *Chemical Physics Letters*, 630:96, 2015.

[66] B. Joalland, T. Mori, T. Martínez, and A. G. Suits. Photochemical dynamics of ethylene cation $C_2H_4^+$. *The Journal of Physical Chemistry Letters*, 5:1467, 2014.

[67] P. Wang, X. Xing, S. Jong Baek, and C. Ng. Rovibrationally selected and resolved pulsed field ionization-photoelectron study of ethylene. *The Journal of Physical Chemistry A*, 108:10035, 2004.

[68] X. Xing, M. Bahng, P. Wang, K. Lau, S. Baek, and C. Ng. Rovibrationally selected and resolved state-to-state photoionization of ethylene using the infrared-vacuum ultraviolet pulsed field ionization-photoelectron method. *The Journal of Chemical Physics*, 125:133304, 2006.

[69] H. Andrei, N. Solcà, and O. Dopfer. IR spectrum of the ethyl cation: Evidence for the nonclassical structure. *Angewandte Chemie International Edition*, 47:395, 2008.

[70] A. M. Ricks, G. E. Douberly, P. R. Schleyer, and M. A. Duncan. Infrared spectroscopy of protonated ethylene: The nature of proton binding in the non-classical structure. *Chemical Physics Letters*, 480:17, 2009.

[71] O. Dopfer, H. Andrei, and N. Solcà. IR spectra of $C_2H_5^+$-N_2 isomers: Evidence for dative chemical bonding in the isolated ethanediazonium ion. *The Journal of Physical Chemistry A*, 115:11466, 2011.

[72] Y. Kurosaki and T. Takayanagi. Ab initio molecular orbital study on the H_2 loss reaction from ethane cation, $C_2H_6^+$. *Chemical Physics Letters*, 277:291, 1997.

[73] J. Walkimar de M. Carneiro, P. von R. Schleyer, M. Saunders, R. Remington, H. F. Schaefer III, A. Rauk, and T. S. Sorensen. Protonated ethane. A theoretical investigation of $C_2H_7^+$ structures and energies. *Journal of American Chemical Society*, 116:3483, 1994.

[74] Y. Kabbadj, T. R. Huet, D. Uy, and T. Oka. Infrared spectroscopy of the amidogen ion, NH_2^+. *Journal of Molecular Spectroscopy*, 175:277, 1996.

[75] S. S. Lee and T. Oka. Diode laser spectroscopy of the ν_2 fundamental and hot bands of NH_3^+. *The Journal of Chemical Physics*, 94:1698, 1991.

[76] M. W. Crofton and T. Oka. Infrared studies of molecular ions. I. The ν_3 band of NH_4^+. *The Journal of Chemical Physics*, 79:3157, 1983.

[77] M. G. Bawendi, B. D. Rehfuss, B. M. Dinelli, M. Okumura, and T. Oka. Observation and analysis of the ν_3 band of NH_3^+. *The Journal of Chemical Physics*, 90:5910, 1989.

[78] C. S. Gudeman, M. H. Begemann, J. Pfaff, and R. J. Saykally. Velocity-modulated infrared laser spectroscopy of molecular ions: The ν_1 band of HNN^+. *The Journal of Chemical Physics*, 78:5837, 1983.

[79] T. J. Sears. Observation of the ν_2 (bending) fundamental of the HN_2^+ ion at 14.6 micrometers. *The Journal of the Optical Society of America B*, 2:786, 1985.

[80] S. C. Foster and A. R. W. McKellar. The ν_3 fundamental bands of HN_2^+, DN_2^+, and DCO^+. *The Journal of Chemical Physics*, 81:3424, 1984.

[81] J. C. Owrutsky, C. S. Gudeman, C. C. Martner, L. M. Tack, N. H. Rosenbaum, and R. J. Saykally. Determination of the equilibrium structure of protonated nitrogen by high-resolution infrared laser spectroscopy. *The Journal of Chemical Physics*, 84:605, 1986.

[82] C. J. Pursell, D. P. Weliky, and T. Oka. Collision-induced double resonance studies of HN_2^+ and HCN. *The Journal of Chemical Physics*, 93:7041, 1990.

[83] W. C. Ho, C. J. Pursell, D. P. Weliky, K. Takagi, and T. Oka. Infrared-microwave double resonance spectroscopy of molecular ions: HN_2^+. *The Journal of Chemical Physics*, 93:87, 1990.

[84] B. E. Turner. U93.174: A new interstellar line with quadrupole hyperfine splitting. *The Astrophysical Journal*, 193:L83, 1974.

[85] S. Green, J. A. Montgomery Jr., and P. Thaddeus. Tentative identification of U93.174 as the molecular ion $N_2H_2^+$. *The Astrophysical Journal*, 193:L89, 1974.

[86] P. Thaddeus and B. E. Turner. Confirmation of interstellar $N_2H_2^+$. *The Astrophysical Journal*, 201:L25, 1975.

[87] R. J. Saykally, T. A. Dixon, T. G. Anderson, P. G. Szanto, and R. C. Woods. Laboratory microwave spectrum and rest frequencies of the N_2H^+ ion. *The Astrophysical Journal*, 205:L101, 1976.

[88] J. Palaudoux and M. Hochlaf. Theoretical investigations of the $N_2H_2^+$ cation and of its reactivity. *The Journal of Chemical Physics*, 121:1782, 2004.

[89] Y. Xie, W. D. Allen, Y. Yamaguchi, and H. F. Schaefer III. Is the oxywater radical cation more stable than neutral oxywater? *The Journal of Chemical Physics*, 104:7615, 1996.

[90] K. C. Sears, J. W. Ferguson, T. J. Dudley, R. S. Houk, and M. S. Gordon. Theoretical investigation of small polyatomic ions observed in inductively coupled plasma mass spectrometry: H_xCO^+ and $H_xN_2^+$ (x = 1, 2, 3). *The Journal of Physical Chemistry A*, 112:2610, 2008.

[91] D. C. Frost, S. T. Lee, C. A. McDowell, and N. P. C. Westwood. The photoelectron spectra of diazene, diazene-d_2, and *trans*-methyldiazene. *The Journal of Chemical Physics*, 64:4719, 1976.

[92] D. Lauvergnat and M. Hochlaf. Theoretical spectroscopy of trans-$HNNH^+$ and isotopomers. *The Journal of Chemical Physics*, 130:224312, 2009.

[93] M. H. Matus, A. J. Arduengo III, and D. A. Dixon. The heats of formation of diazene, hydrazine, $N_2H_3^+$, $N_2H_5^+$, N_2H, and N_2H_3 and the methyl derivatives CH_3NNH, CH_3NNCH_3, and $CH_3HNNHCH_3$. *The Journal of Physical Chemistry A*, 110:10116, 2006.

[94] K. Osafune, S. Katsumata, and K. Kimura. Photoelectron spectroscopic study of hydrazine. *Chemical Physics Letters*, 19:369, 1973.

[95] M. Habas, I. Baraille, C. Larrieu, and M. Chaillet. Ab initio calculation of the electronic spectrum and ionization potentials of hydrazine. *Chemical Physics*, 219:63, 1997.

[96] J. C. Decius and D. P. Pearson. The infrared absorption of crystalline and liquid hydrazine monochloride and monobromide. *Journal of the American Chemical Society*, 75:2436, 1953.

[97] J. M. Robbe, M. Monnerville, G. Chambaud, P. Rosmus, and P. J. Knowles. Theoretical spectroscopic data of the HO_2^+ ion. *Chemical Physics*, 252:9, 2000.

[98] G. E. Quelch, Y. Xie, B. F. Yates, Y. Yamaguchi, and H. F. Schaefer III. The HO_2^+ ion. *Molecular Physics*, 68:1095, 1989.

[99] R. N. Barnett and U. Landman. Structure and energetics of ionized water clusters: $(H_2O)_n^+$, n = 2−5. *The Journal of Physical Chemistry A*, 101:164, 1997.

[100] H. Do and N. A. Besley. Structure and bonding in ionized water clusters. *The Journal of Physical Chemistry A*, 117:5385, 2013.

[101] H. Shinohara, N. Nishi, and N. Washida. Photoionization of water clusters at 11.83 eV: Observation of unprotonated cluster ions $(H_2O)_n^+$ (2≤n≤10). *The Journal of Chemical Physics*, 84:5561, 1986.

[102] C. A. Kauffman. The nuclear spin dependence of the reaction of H_3^+ with H_2 and the proposed spectroscopic investigation of HO_2^+. Master's thesis, University of Illinois, 2011.

[103] S. A. Nizkorodov, D. Roth, R. V. Olkhov, J. P. Maier, and O. Dopfer. Infrared predissociation spectra of He−HO_2^+ and Ne−HO_2^+: prediction of the ν_1 frequency of HO_2^+. *Chemical Physics Letters*, 278:26, 1997.

[104] G. de Petris, A. Cartoni, R. Cipollini, and A. Troiani. A novel route to $H_2O_2^+$ ions via direct generation of the oxywater cation H_2OO^+. *International Journal of Mass Spectrometry*, 249:311, 2006.

[105] W. E. Thompson, C. L. Lugez, and M. E. Jacox. The infrared spectrum of $HOOH^+$ trapped in solid neon. *The Journal of Chemical Physics*, 137:144305, 2012.

[106] S. P. de Visser, L. J. de Koning, and N. M. M. Nibbering. Reactivity and thermochemical properties of the water dimer radical cation in the gas phase. *The Journal of Physical Chemistry*, 99:15444, 1995.

[107] S. Tomoda, Y. Achiba, and K. Kimura. Photoelectron spectrum of the water dimer. *Chemical Physics Letters*, 87:197, 1982.

[108] G. H. Gardenier, M. A. Johnson, and A. B. McCoy. Spectroscopic study of the ion−radical H-bond in $H_4O_2^+$. *The Journal of Physical Chemistry A*, 113:4772, 2009.

[109] T. D. Fridgen, T. B. McMahon, L. MacAleese, J. Lemaire, and P. Maitre. Infrared spectrum of the protonated water dimer in the gas phase. *The Journal of Physical Chemistry A*, 108:9008, 2004.

[110] K. R. Asmis, N. L. Pivonka, G. Santambrogio, and M. Br˙Gas-phase infrared spectrum of the protonated water dimer.

[111] O. Vendrell, F. Gatti, and H. Meyer. Full dimensional (15-dimensional) quantum-dynamical simulation of the protonated water dimer. II. Infrared spectrum and vibrational dynamics. *The Journal of Chemical Physics*, 127:184303, 2007.

[112] L. I. Yeh, M. Okumura, J. D. Myers, J. M. Price, and Y. T. Lee. Vibrational spectroscopy of the hydrated hydronium cluster ions $H_3O^+ \cdot (H_2O)_n$ (n = 1, 2, 3). *The Journal of Chemical Physics*, 91:7319, 1989.

[113] K. L. Aplin and R. A. McPheat. Absorption of infra-red radiation by atmospheric molecular cluster-ions. *Journal of Atmospheric and Solar-Terrestrial Physics*, 67:775, 2005.

[114] J. Dai, Z. Bačić, X. Huang, S. Carter, and J. M. Bowman. A theoretical study of vibrational mode coupling in $H_5O_2^+$. *The Journal of Chemical Physics*, 119:6571, 2003.

[115] M. Dagrada, M. Casula, A. M. Saitta, S. Sorella, and F. Mauri. Quantum Monte Carlo study of the protonated water dimer. *Journal of Chemical Theory and Computation*, 10:1980, 2014.

[116] L. I. Yeh, Y. T. Lee, and J. T. Hougen. Vibration-rotation spectroscopy of the hydrated hydronium ions $H_5O_2^+$ and $H_9O_4^+$. *Journal of Molecular Spectroscopy*, 164:473, 1994.

[117] F. Agostini, R. Vuilleumier, and G. Ciccotti. Infrared spectroscopy and effective modes analysis of the protonated water dimer $H^+(H_2O)_2$ at room temperature under H/D substitution. *The Journal of Chemical Physics*, 134:84303, 2011.

[118] M. Bogey, C. Demuynck, and J. L. Destombes. Millimeter and submillimeter wave spectrum of protonated hydrocyanic acid ($HCNH^+$). *The Journal of Chemical Physics*, 83:3703, 1985.

[119] L. M. Ziurys and B. E. Turner. $HCNH^+$: A new interstellar molecular ion. *The Astrophysical Journal*, 302:L31, 1986.

[120] R. S. Altman, M. W. Crofton, and T. Oka. High resolution infrared spectroscopy of the ν_1 (NH stretch) and ν_2 (CH stretch) bands of $HCNH^+$. *The Journal of Chemical Physics*, 81:4255, 1984.

[121] R. S. Altman, M. W. Crofton, and T. Oka. Observation of the infrared ν_2 band (CH stretch) of protonated hydrogen cyanide, $HCNH^+$. *The Journal of Chemical Physics*, 80:3911, 1984.

[122] M. Kajita, K. Kawaguchi, and E. Hirota. Diode laser spectroscopy of the ν_3 (CN stretch) band of protonated hydrogen cyanide. *Journal of Molecular Spectroscopy*, 127:275, 1988.

[123] D. J. Liu, S. T. Lee, and T. Oka. The ν_3 fundamental band of $HCNH^+$ and the $2\nu_3 \leftarrow \nu_3$ and $\nu_2 + \nu_3 \leftarrow \nu_2$ hot bands of HCO^+. *Journal of Molecular Spectroscopy*, 128:236, 1988.

[124] K. Tanaka, K. Kawaguchi, and E. Hirota. Diode laser spectroscopy of the ν_4 (HCN bend) band of ($HCNH^+$). *Journal of Molecular Spectroscopy*, 117:408, 1986.

[125] W. C. Ho, C. E. Blom, D. J. Liu, and T. Oka. The infrared ν_5 band (HNC bend) of protonated hydrogen cyanide, $HCNH^+$. *Journal of Molecular Spectroscopy*, 123:251, 1987.

[126] V. Brites and L. Jutier. New *ab initio* study of the spectroscopy of $HCNH^+$. *Journal of Molecular Spectroscopy*, 271:25, 2012.

[127] K. A. Peterson, R. C. Mayrhofer, and R. C. Woods. Configuration interaction spectroscopic properties of $X^2\sigma^+$, HNC^+, and $X^2\pi$ HCN^+. *The Journal of Chemical Physics*, 93:4946, 1990.

[128] D. Forney, W. E. Thompson, and M. E. Jacox. The vibrational spectra of molecular ions isolated in solid neon. IX. HCN^+, HNC^+, and CN^-. *The Journal of Chemical Physics*, 97:1664, 1992.

[129] F. Holzmeier, M. Lang, K. Hader, P. Hemberger, and I. Fischer. H_2CN^+ and H_2CNH^+: New insight into the structure and dynamics of mass-selected threshold photoelectron spectra. *The Journal of Chemical Physics*, 138:214310, 2013.

[130] P. C. Burgers, J. L. Holmes, and J. K. Terlouw. Gaseous $[H_2, C, N]^+$ $[H_3, C, N]^+$ ions. Generation, heat of formation, and dissociation characteristics of $[H_2CN]^+$, $[HCNH^+]$, $[CNH_2]^+$, $[H_2CNH]^+$, and $[HCNH_2]^+$. *Journal of the American Chemical Society*, 106:2762, 1984.

[131] M. T. Nguyen, J. Rademakers, and J. M. L. Martin. Concerning the heats of formation of the $[C, H_3, N]^+$ radical cations. *Chemical Physics Letters*, 221:149, 1994.

[132] J. Zhou and H. B. Schlegel. Ab initio classical trajectory study of the dissociation of neutral and positively charged methanimine (CH_2NH^{n+} n=0−2. *The Journal of Physical Chemistry A*, 113:9958, 2009.

[133] P. B. Davies, P. A. Hamilton, and W. J. Rothwell. Infrared laser spectroscopy of the ν_3 fundamental of HCO^+. *The Journal of Chemical Physics*, 81:1598, 1984.

[134] D. Buhl and L. E. Snyder. Unidentified interstellar microwave line. *Nature*, 228:5268, 1970.

[135] W. Klemperer. Carrier of the interstellar 89.190 GHz line. *Nature*, 227:1230, 1970.

[136] R. C. Woods, T. A. Dixon, R. J. Saykally, and P. G. Szanto. Laboratory microwave spectrum of HCO^+. *Physical Review Letters*, 35:1269, 1975.

[137] R. C. Woods, R. J. Saykally, T. G. Anderson, T. A. Dixon, and P. G. Szanto. The molecular structure of HCO^+ by the microwave substitution method. *The Journal of Chemical Physics*, 75:4256, 1981.

[138] C. S. Gudeman, M. H. Begemann, J. Pfaff, and R. J. Saykally. Velocity-modulated infrared laser spectroscopy of molecular ions: The ν_1 band of HCO^+. *Physical Review Letters*, 50:727, 1983.

[139] T. Amano. The ν_1 fundamental band of HCO^+ by difference frequency laser spectroscopy. *The Journal of Chemical Physics*, 79:3595, 1983.

[140] V. Lattanzi, A. Walters, B. J. Drouin, and J. C. Pearson. Rotational spectrum of the formyl cation, HCO^+, to 1.2 THz. *The Astrophysical Journal*, 662:771, 2007.

[141] T. Amano and H. E. Warner. Laboratory detection of protonated formaldehyde (H_2COH^+). *The Astrophysical Journal*, 342:L99, 1989.

[142] J. D. Mosley, T. C. Cheng, A. B. McCoy, and M. A. Duncan. Infrared spectroscopy of the mass 31 cation: Protonated formaldehyde vs methoxy. *The Journal of Physical Chemistry A*, 116:9287, 2012.

[143] D. Chomiak, A. Taleb-Bendiab, S. Civiš, and T. Amano. Millimeter-wave laboratory detection of H_2COH^+. *The International Symposium on Molecular Spectroscopy*, The Ohio State University:Columbus, OH, 1994.

[144] L. Dore, G. Cazzoli, S. Civiš, and F. Scappini. Extended measurements of the millimeter wave spectrum of H_2COH^+. *Chemical Physics Letters*, 244:145, 1995.

[145] M. Ohishi, S. Ishikawa, T. Amano, H. Oka, W. M. Irvine, J. E. Dickens, L. M. Ziurys, and A. J. Apponi. Detection of a new interstellar molecular ion, H_2COH^+ (protonated formaldehyde). *The Astrophysical Journal*, 471:L61, 1996.

[146] M. W. Porambo. Molecular ion spectroscopy: New methods and the proposed study of H_2CO^+. *Research Prospectus for Preliminary Examination*, University of Illinois, 2011.

[147] B. Niu, D. A. Shirley, and Y. Bai. High resolution photoelectron spectroscopy and femtosecond intramolecular dynamics of H_2CO^+ and D_2CO^+. *The Journal of Chemical Physics*, 98:4377, 1993.

[148] P. J. Bruna, M. R. Hachey, and F. Grein. The electronic structure of the H_2CO^+ radical and higher Rydberg states of H_2CO. *Molecular Physics*, 94:917, 1998.

[149] A. M. Schulenburg, M. Meisinger, P. P. Radi, and F. Merkt. The formaldehyde cation: Rovibrational energy level structure and Coriolis interaction near the adiabatic ionization threshold. *Journal of Molecular Spectroscopy*, 250:44, 2008.

[150] R. T. Wiedmann, M. G. White, K. Wang, and V. McKoy. Rotationally resolved photoionization of polyatomic hydrides: CH_3, H_2O, H_2S, H_2CO. *The Journal of Chemical Physics*, 100:4738, 1994.

[151] S. Kuo, Z. Zhang, S. K. Ross, R. B. Klemm, R. D. Johnson, P. S. Monks, Jr. R. P. Thorn, and L. J. Stief. Discharge flow-photoionization mass spectrometric study of HNO: Photoionization efficiency spectrum and ionization energy and proton affinity of NO. *The Journal of Physical Chemistry A*, 101:4035, 1997.

[152] J. Baker, V. Butcher, J. M. Dyke, and A. Morris. Vacuum ultraviolet photoelectron spectroscopic study of the NH_2O and HNO molecules. *Journal of the Chemical Society, Faraday Transactions*, 86:3843, 1990.

[153] A. B. Houria, H. Gritli, N. Jaidane, Z. B. Lakdhar, G. Chambaud, and P. Rosmus. Electronic states of HNO^+ and HON^+. *Chemical Physics*, 274:71, 2001.

[154] D. Schr˙ Experimental and ab initio MO studies on $[H_2,N,O]^+$ ions in the gas phase: Characterization of the isomers H_2NO^+, $HNOH^+$, and NOH_2^+ and the mechanism of unimolecular dehydrogenation of $[H_2,N,O]^+$.

[155] F. Grandinetti, J. Hrušák, and D. Schr˙ Gas-phase protonation of nitrosyl hydride: A Gaussian-1 ab initio MO study of the structure, stability, and unimolecular interconversion processes of various $[H_2,N,O]^+$ isomers.

[156] P. J. Bruna and C. M. Marian. Ab initio study on the isomers of HNO^+ and NOH^+, vertical spectra and heat of formation. *Chemical Physics*, 37:425, 1979.

[157] A. A. Mills. *Design, Construction, and Characterization of an Ultra-sensitive, High-precision Fast Ion-Beam Spectrometer for the Study of Molecular Ions*. PhD thesis, The University of Illinois, 2011.